Naval Research Laboratory
Washington, DC 20375-5320

NRL/5310/MR—2023/5

Method of Characteristics Applied to Stochastic Maxwell's Equations in the Homogeneous Chaos Basis Expansion

DAVID R. BERGMAN

Radar Analysis Branch
Radar Division

October 17, 2023

REPORT DOCUMENTATION PAGE

Form Approved OMB No. 0704-0188

1. REPORT DATE *(DD-MM-YYYY)* 17-10-2023	**2. REPORT TYPE** NRL Memorandum Report	**3. DATES COVERED** *(From - To)* 10/3/22– 9/15/23

4. TITLE AND SUBTITLE Method of Characteristics Applied to Stochastic Maxwell's Equations in the Homogeneous Chaos Basis Expansion	**5a. CONTRACT NUMBER**
	5b. GRANT NUMBER
	5c. PROGRAM ELEMENT NUMBER 61153N
6. AUTHOR(S) David R. Bergman	**5d. PROJECT NUMBER**
	5e. TASK NUMBER EW021-05-43
	5f. WORK UNIT NUMBER 1AA1
7. PERFORMING ORGANIZATION NAME(S) AND ADDRESS(ES) Naval Research Laboratory 4555 Overlook Avenue, SW Washington, DC 20375-5320	**8. PERFORMING ORGANIZATION REPORT NUMBER** NRL/5310/MR--2023/5
9. SPONSORING / MONITORING AGENCY NAME(S) AND ADDRESS(ES) Office of Naval Research One Liberty Center 875 North Randolph Street Arlington, VA 22203-1995	**10. SPONSOR / MONITOR'S ACRONYM(S)** ONR
	11. SPONSOR / MONITOR'S REPORT NUMBER(S)

12. DISTRIBUTION / AVAILABILITY STATEMENT

DISTRIBUTION STATEMENT A: Approved for public release; distribution is unlimited.

13. SUPPLEMENTARY NOTES

14. ABSTRACT

The method of characteristics is applied to the stochastic Maxwell's equations (SME) expressed in both vector and differential form format. Stochastic effects are included using the homogeneous polynomial chaos. It is demonstrated that the SME contains an infinite number of light cone or null hyper-surface structures each with a wave speed determined by the eigenvalues of the stochastic permittivity and/or permeability. The stochastic solutions can be expressed in terms of these independent propagating modes.

15. SUBJECT TERMS

Electrodynamics   Stochastic differential equations   Method of characteristics
Differential geometry   Ray Theory

16. SECURITY CLASSIFICATION OF:			**17. LIMITATION OF ABSTRACT**	**18. NUMBER OF PAGES**	**19a. NAME OF RESPONSIBLE PERSON** David Bergman
a. REPORT U	**b. ABSTRACT** U	**c. THIS PAGE** U	U	61	**19b. TELEPHONE NUMBER** *(include area code)* (202) 934-4820

Standard Form 298 (Rev. 8-98)
Prescribed by ANSI Std. Z39.18

This page intentionally left blank.

CONTENTS

METHOD OF CHARACTERISTICS APPLIED TO STOCHASTIC MAXWELL'S EQUATIONS IN THE HOMOGENEOUS CHAOS BASIS EXPANSION

1. INTRODUCTION

1.1 General Introduction

This report presents the first year's result of a three-year 6.1 new-start base program entitled "Investigation of the relation between stochastic differential geometry and stochastic differential equations for application to RCS prediction". The long term effort seeks to understand how the disciplines of differential geometry and stochastic partial differential equations (SPDE) intersect with an emphasis on Maxwell's equations. One motivation is a desire to capitalize on the well-known connection between geodesics (ray paths) and the full solution to a PDE system as dictated by the method of characteristics. Another motivation is to explore the variety of methods and techniques for developing SPDEs, especially those involving stochastic derivative operators. Lastly, research problems in stochastic wave propagation and uncertainty quantification (UQ) frequently start from a reduced form of Maxwell's equations, *e.g.* the parabolic or ray equation. The position taken in this research effort is that all approaches considered will originate from Maxwell's equations, proceeding initially without approximation, to develop final results in a logical and systematic manner.

The connection between ray paths and waves (fields in general) is a cornerstone of the classical theory of PDEs. The introduction of stochasticity, either by fluctuations in the environment or uncertainty in fixed parameters (treated as random variables (RV)), increases the complexity of the problem, and, in some cases, could make classical approaches difficult to apply and interpret, or worse invalid. Moving forward this research will touch the following topics:

- General theory of PDE
- Theory of characteristics
- Ray theory
- Geodesic flows on pseudo-Riemannian manifolds
- Optics
- Electrodynamics
- Maxwell's equations
- Stochastic calculus
- Stochastic PDE (SPDE)
- Stochastic manifolds
- The effect of environmental fluctuations on wave propagation
- Uncertainty Quantification

The main thrust is ray theory but all results will be derived from Maxwell's equations to ensure consistency, and to ballast results with a first principles approach. This report provides a full description of the polynomial chaos basis applied to Maxwell's equations, the result of applying the method of characteristics to the resulting stochastic version of Maxwell's equations with an interpretation of the results, and a discussion of the implications to UQ analysis of electromagnetic wave propagation in stochastic media.

Manuscript approved October 17, 2023.

1.2 Technical Introduction

Historically, the idea of rays predates both Maxwell's equations and the method of characteristics. Newton viewed light as being made of particles, "corpuscles", which traveled along trajectories that minimized travel time between two points in space, Fermat's principle [1]. Given the Newtonian view of space and time, these paths (rays) are straight lines when the medium of propagation is homogeneous. Using a ray path view of light one can understand the general behavior of reflection and refraction at a boundary between two homogeneous media. The study of light from this perspective is the discipline of optics. The behavior of ray paths can be summarized by the following two equations,

$$\delta\tau_{(a,b)} = 0 \tag{1.1}$$

$$\tau_{(a,b)} = \int_a^b \frac{ds}{c} \tag{1.2}$$

Equation (1.1) states that the total travel time between points a and b, $\tau_{(a,b)}$, is an extrema under variation of path near the critical path while equation (1.2) defines the travel time as the integral along the path, with the parameter *s* representing 3-dimensional (3D) arc length. Equation (1.2) can also be expressed in terms of the index of refraction, $\tau_{(a,b)} = \int_a^b n\,dt$. When the medium is inhomogeneous, the refractive index may be a function of position and time, $\tau_{(a,b)} = \int_a^b n(\vec{x},t)\,dt$. In this more general case, ray paths are no longer straight lines, but rather solutions to a more general ray path equation that is well known in optics and acoustics [2, 3]. It is worth noting that the general ray path equation is a geodesic equation related to a metric tensor induced by the local refractive index and other material properties [4-6]. This point will be elaborated on in later sections of the report.

Throughout the 1700s and 1800s physicists explored and documented numerous phenomena related to electricity and magnetism, treated as separate phenomena, later unified by the work of Faraday and Maxwell. Maxwell's equations provide a complete, unified, description of all classical electric and magnetic phenomena. It was further demonstrated that propagating solutions, made of oscillating electric and magnetic field vectors, to Maxwell's equations exist providing a theoretical basis for light as an electromagnetic wave. This accomplishment brought optics under the umbrella of electrodynamics as a predicted result rather than an independent field of study. In fact, all that is known about ray path geometry can be derived from Maxwell's equations using one of two approaches; (1) the high frequency expansion of an ansatz of the form $A(\vec{x},t)\exp\big(i\theta(\vec{x},t)\big)$, or (2) by applying the method of characteristics used in the study of PDEs to Maxwell's equations [7].

It is often necessary to model systems or solve problems where the input parameters of the system equations are unknown or take values in some range described by a probability distribution. An example might be a medium with a refractive index in the interval [1.1, 1.3] obeying a uniform distribution. A more complex example is a height dependent refractive index expressed in terms of polynomials of order m, $P_m(z)$, $n(z) = \sum a_m P_m(z)$ with the constants $\{a_m\}$ each given by a random draw. Each choice of $\{a_m\}$ creates a different environmental model and will produce distinct solutions for a propagating electromagnetic field and different ray paths. Given information about the $\{a_m\}$ and their probability density function (pdf) the problem is to quantify the expected statistical behavior of the outputs of the system, in this case $\vec{E}(\vec{x},t)$ and $\vec{B}(\vec{x},t)$, or perhaps travel time between any two points (*e.g.* a transmitter and receiver). This is referred to as UQ. Given the stochastic nature of the parameters it is necessary to develop a stochastic method for studying Maxwell's equations.

A standard approach in many fields of research is to assume the ray equation is valid regardless of its relation to the original PDE and apply randomness to the local refractive profile. This approach assumes that a ray path description makes sense as a first cause rather than connecting it to the field equations that naturally predict the existence of rays. It also assumes that the connection between a PDE and its characteristics remains the same when the PDE is elevated to an SPDE. I can find no derivation in the literature that proves this as a general rule. McDaniel and Mahalov, for example, comment that rays can be derived from Fermat's principal and develop stochastic models of environmental effects on ray path fluctuations [8]. This is a valid position from a purely mathematical point of view, but in light of the fact that Maxwell's equations are now understood to describe optics it seems unnatural to start from an approximate description, or one that may not even follow from first principles. It is not the goal of this report to demonstrate that existing approaches are wrong, but to start from Maxwell's equations and see where the math leads after applying steps in a logical order. If they produce the same result then great, there is proof that treating rays as fundamental objects in stochastic analysis is valid. Otherwise, the difference needs to be explored, understood, and completely quantified in later reports.

Many UQ studies make use of either:

(1) Developing large Monte Carlo data sets using the original equations and random draws on the set of uncertain input parameters,
(2) Deriving expressions for the auto and cross correlation of the output fields using the original equations by averaging over an assumed pdf.

An alternative method considered here is the use of polynomial chaos basis, developed by N. Wiener in 1938 [9]. This approach expands all input parameters and output fields in terms of an infinite series using an orthonormal basis for a Hilbert space; see equation (1.3) for the expansion of a scalar function of one variable.

$$f(x) = \sum_{n=0}^{\infty} a_n(x)\Phi_n(\theta) \tag{1.3}$$

This approach leads to replacing a finite number of fields with an infinite set of fields that may become coupled through the stochastic parameters or non-linearity. It may seem like the problem is now more complex and difficult to solve but there are known advantages to this approach.

(1) Despite having an infinite number of terms, case studies illustrate that one can get numerical convergence with a small finite number of terms. Thus one can accurately characterize the statistics of the system in much less time and using less computational resources than running Monte Carlo (MC) cases thousands of times.
(2) Solving the chaos system, even approximately, provides a complete description of the statistics of the outputs whereas other approaches only describe second order statistics, *i.e.* correlation matrix.
(3) The chaos approach leads to a set of equations for smooth, differentiable, functions whereas other approaches (not elaborated on here) may introduce discontinuous processes.

The structure of this report is as follows. Chapter 2 provides a complete presentation of Maxwell's equations with inhomogeneous and anisotropic medium properties in multiple representations. Chapter 3 applies the polynomial chaos basis to a specific choice of Maxwell's equations with inhomogeneous material properties. At this point the stochastic Maxwell equation (SME) could be prototyped and used as a numeric SPDE. Chapter 4 applies the method of characteristics to the resulting equation in chapter 3 and derives the equations for the bicharacteristic curves of the SME. Chapter 5 presents an interpretation of the results of chapter 4. Finally, chapter 6 discusses the theoretical implications of the results and compares the main result of this report to the same if it were applied to the ray equations from the start. It will be shown that the two approaches do not lead to the same system for describing stochastic ray theory. This sets the stage for future efforts on this program and future reports. To make the chapters easier to read the content focuses more on presenting results with full description of their impact. Some derivation steps may be provided if they are deemed important and do not distract from the main point of the text. Details are documented in the appendices at the end of the report.

2. MAXWELL'S EQUATIONS

2.1 Multiple representations in vector notation

The starting point is Maxwell's equations in the presence of bulk dielectric and magnetic materials and free charge sources, following the notation of Jackson [10],

$$\vec{\nabla}\cdot\vec{D} = \rho_f \tag{2.1}$$

$$\vec{\nabla}\cdot\vec{B} = 0 \tag{2.2}$$

$$\vec{\nabla}\times\vec{E} + \frac{\partial\vec{B}}{\partial t} = 0 \tag{2.3}$$

$$\vec{\nabla}\times\vec{H} - \frac{\partial\vec{D}}{\partial t} = \vec{J}_f \tag{2.4}$$

In equations (2.1) through (2.4), the subscript f refers to "free", free charge and free current. The vectors $\vec{E}$ and $\vec{D}$ are electric field and electric displacement field respectively. The pseudo-vectors, $\vec{B}$ and $\vec{H}$, are the magnetic induction and the macroscopic magnetic field respectively. These fields are related by a set of constitutive equations.

$$\vec{D} = \varepsilon\vec{E} \tag{2.5}$$

$$\vec{H} = \frac{1}{\mu}\vec{B} \tag{2.6}$$

The parameter ε (μ) is the electric permittivity (magnetic permeability) of the material. When the material is free space $\varepsilon = \varepsilon_0$ and $\mu = \mu_0$. These quantities are also defined in terms of relative permittivity (permeability) or the dielectric constant ($\kappa = \varepsilon/\varepsilon_0$) and magnetic susceptibility ($\chi_m = \mu/\mu_0 - 1$). One frequently encounters complex versions of these quantities in lossy materials, *e.g.* $\kappa = \kappa' - i\sigma/\omega\varepsilon_0$, where σ is the dielectric conductivity. In the most general circumstances, the material parameters are tensors, indicating the medium contains anisotropic properties, which depend on position, time, frequency and local field strength in the case of non-linear materials. For anisotropic media, equations (2.5) and (2.6) are replaced with tensor (or matrix) relationships, presented below in component form.

$$D_j = \varepsilon_{ji} E_i \tag{2.7}$$

$$B_j = \mu_{ji} H_i \tag{2.8}$$

Several advances in computational electromagnetics and propagation start with equations 2.1-2.4 and some simplifying assumptions to arrive at a second order "wave equation" that decouples $\vec{E}$ and $\vec{B}$. This serves as a foundation for many parabolic approximations [11].

This report will use a representation of Maxwell's equations that treats $\vec{D}$ and $\vec{B}$ as the independent fields but could have just as well started with $\vec{E}$ and $\vec{H}$ as the independent field and ε and μ as the stochastic input parameters. The specific choice made here is a matter of convenience and the main results hold regardless of the representation. In practice the choice would be driven by which parameters are easily measured or that have a simple pdf.

2.2 Maxwell's equations in differential form representation

The vector representation on electromagnetism was developed by Heaviside and has become the most popular representation for teaching and working in Electrodynamics. Around the same time, Cartan developed an alternate representation using differential forms and exterior calculus. Historically, the vector representation seems to have dominated engineering and physics, but in modern theoretical physics the differential form representation is generally considered more appropriate and to some extent more correct. Using tensor notation makes the unification of electricity and magnetism more apparent, as well as the existence of Lorentz invariance. Lastly, the presence of gauge invariance is demonstrated very simply using exterior calculus via the statement $\mathrm{d}F = 0$, which reads "the field tensor is a closed 2-form" leading to the result $F = \mathrm{d}A$ under certain topological restrictions [12]. It is unfortunate that the exterior calculus version of Maxwell's equations has been seen in engineering disciplines as esoteric for well over 100 years, but recent trends in electrical engineering are working to correct this [13-15]. This section presents the differential forms version of Maxwell's equations and relates them to the vector form in section 2.1.

The differential form representation begins with the fact that the electric and magnetic field can be expressed as components of an antisymmetric second rank tensor, the electromagnetic field tensor, equation (2.9).

$$F_{\mu\nu} = \begin{bmatrix} 0 & E_x & E_y & E_z \\ -E_x & 0 & B_z & -B_y \\ -E_y & -B_z & 0 & B_x \\ -E_z & B_y & -B_x & 0 \end{bmatrix} \tag{2.9}$$

Greek indices range from 0 to 3 with 0 corresponding to the time coordinate, and 1, 2, 3 corresponding to spatial coordinates. In a local coordinate basis, the following geometric invariant quantity is defined.

$$F = \frac{1}{2} F_{\mu\nu} dx^{\mu} \wedge dx^{\nu} \tag{2.10}$$

The wedge product, $dx^{\mu} \wedge dx^{\nu}$, is antisymmetric by definition, *e.g.* $d\mathrm{x} \wedge dy = -dy \wedge dx$, $dx \wedge dx = 0$ *etc*. Details on this notation and the algebra of p-forms can be found in reference [16]. In this notation, using exterior calculus, Maxwell's two homogeneous equations, (2.2) and (2.4), are expressed very succinctly.

$$dF = 0 \tag{2.11}$$

The free charge and current density are combined into a space-time vector (4-vector).

$$\boldsymbol{J}^{\mu} = \begin{bmatrix} -\rho_f \\ \vec{J}_f \end{bmatrix} \tag{2.12}$$

The second set of Maxwell's equations, the inhomogeneous set consisting of (2.1) and (2.3), are constructed by applying the Hodge operator to the field tensor (2.9) along with a few additional steps.

$$\star\, d \star F = \boldsymbol{J} \tag{2.13}$$

The Hodge star operator applied to a *p*-form generates a "dual" (*n*-*p*)-form where *n* = the dimension of the manifold. In this case $\star$ maps $\vec{E} \to -\vec{B}$ and $\vec{B} \to \vec{E}$. Equations (2.11) and (2.13) contain all four of Maxwell's equations, (2.1)–(2.4) in the case when the medium is free space (or more generally an infinite homogeneous medium). Equation (2.11) states that the field tensor is a closed 2-form which means it can be expressed as the derivative of a form of one lower order, *i.e.* $F = dA$ with $A = A_{\mu} dx^{\mu}$. In a source free region of space, the dual field tensor $\star F$ is also closed, $d \star F = 0$. The second order equations for A are $d^2 A = 0$ and $d \star dA = 0$. The first is an identity and the second provides free propagation solutions.

The reader may be wondering what happened to the material parameters. Theorists will likely have assumed they are set to 1, or absorbed into a redefinition of the fields. When they are constant this is harmless. In short, the Hodge operator has information about the metric tensor of the manifold encrypted within it. In certain cases, in the presence of an inhomogeneous material, the material parameters create an effective metric tensor and the entire system can be mapped to "free propagation" on a curved space-time. This type of reframing a system is not new. All of acoustics in a moving fluid can be mapped to a scalar field propagating on a curved manifold where the local refractive index and fluid motion generate the metric tensor [4-6]. O.N. Pin has demonstrated that Newtonian mechanics of conservative systems are equivalent to geodesic flows on Riemannian manifolds where the potential energy creates an effective metric [17]. It is worth noting that the homogeneous set of equations, equation (2.11), are not coupled to the effective metric in any way. Regardless of the nature of the medium, one always has $F = dA$ with some topological constraints. The presence of inhomogeneous permittivity and permeability make a 4-dimensional geometric view somewhat difficult. If one recasts equation (2.11) as two separate equations using differential forms in 3-dimensional space with time treated separately, the magnetic and electric parameters can be absorbed into Hodge operators. This approach has been applied to electromagnetism with inhomogeneous materials by Deschamps in a seminal IEEE article [13].

Equations (2.11) and (2.13) may seem like nothing more than notational convenience, but they reflect the true nature of the electromagnetic field and the source terms. Charge density is not a scalar density but the time component of a 4-vector. Just as time and space coordinates mix under a Lorentz transform, the electric and magnetic field, and the charge and current densities, mix in a specific way.

This section ends by delving deeper into the details of equation (2.13). The correct set of fields in (2.11) is $\vec{E}$ and $\vec{B}$. In the presence of bulk media the second set of equations uses the mapping $\vec{E} \rightarrow -\vec{H} = -R\vec{B}$ and $\vec{B} \rightarrow \vec{D} = \varepsilon\vec{E}$ in the field tensor and applying the exterior derivative to the result. A similar operation can be applied again to the result or to the current on the right hand side. The Hodge star operator takes care of the dual mapping including the relative sign. The material parameters need to be carried over by hand. The result of these operations is denoted by $\tilde{F}$.

$$\tilde{F}_{\mu\nu} = \begin{bmatrix} 0 & -H_x & -H_y & -H_z \\ H_x & 0 & D_z & -D_y \\ H_y & -D_z & 0 & D_x \\ H_z & D_y & -D_x & 0 \end{bmatrix} \tag{2.14}$$

The differential form representation is almost as old as the vector notation introduced by Heaviside, and for many reasons, it is considered the "correct" way of writing Maxwell's equations. Despite this, it has been difficult to convert practitioners in all fields of science and engineering to this paradigm, and the vector notation remains a standard in both the educational and professional fields. It was introduced to electrical engineering in 1981 by Deschamps in a seminal IEEE article [13]. A team at Brigham Young University, Warnick, Selfridge and Arnold has devoted effort to rewriting the electromagnetic theory curriculum to use differential forms rather than vectors (or at the very least introduce the basic mechanics of *p*-forms) [18]. Recent work by many other authors demonstrates the usefulness of forms over vectors in several practical problems in electrical engineering including those with stochasticity [13-15], [18-23].

2.3 Four-vector potential

Using the fact that $F = dA$ with $A = A_\mu dx^\mu$, a consequence of $dF = 0$, the second set of Maxwell's equations can be reduced to an equation for the components of A. The space-time version of this potential is more commonly written in terms of a "scalar" and "vector" potential.

$$A = \psi dt + A_i dx^i \tag{2.15}$$

The quotes around the terms *scalar* and *vector* are well deserved as they are not independent quantities at all, but mix under the action of a Lorentz transformation. Strictly speaking, the differential forms view is the best way to work with gauge theories. Despite this and the comments at the end of the last section, I present the gauge equations in vector form as most readers will be more familiar with them. The magnetic and electric fields are expressed in terms of the components of Eq. (2.15).

$$\vec{B} = \vec{\nabla} \times \vec{A} \tag{2.16}$$

$$E = -\vec{\nabla}\psi - \frac{\partial \vec{A}}{\partial t} \tag{2.17}$$

Inserting these into Eqs. (2.1) and (2.4) and using the constitutive equations leads to the following set of second order equations for the potential functions.

$$\varepsilon\vec{\nabla}\cdot\left[\vec{\nabla}\psi+\frac{\partial\vec{A}}{\partial t}\right]+\vec{\nabla}\varepsilon\cdot\left[\vec{\nabla}\psi+\frac{\partial\vec{A}}{\partial t}\right]+\rho_f=0 \quad (2.18)$$

$$R\left[\vec{\nabla}\left(\vec{\nabla}\cdot\vec{A}\right)-\nabla^2\vec{A}\right]+\vec{\nabla}R\times\left[\vec{\nabla}\times\vec{A}\right]+\frac{\partial\varepsilon}{\partial t}\left[\vec{\nabla}\psi+\frac{\partial\vec{A}}{\partial t}\right]+\varepsilon\frac{\partial}{\partial t}\left[\vec{\nabla}\psi+\frac{\partial\vec{A}}{\partial t}\right]-\vec{J}_f=0 \quad (2.19)$$

The only steps taken are (1) distribute the derivative operators by the Leibnitz rules to expose highest order derivatives, (2) application of the vector identity $\vec{\nabla}\times\left[\vec{\nabla}\times\vec{A}\right]=\vec{\nabla}\left(\vec{\nabla}\cdot\vec{A}\right)-\nabla^2\vec{A}$, and (3) move the source terms to the left hand side (lhs). To study the characteristics of this set of equations only the highest order derivative terms are required. Rearranging leads to the following.

$$\varepsilon\left[\nabla^2\psi+\frac{\partial\vec{\nabla}\cdot\vec{A}}{\partial t}\right]+\mathrm{LOT}=0 \quad (2.20)$$

$$\varepsilon\vec{\nabla}\left(\frac{\partial\psi}{\partial t}\right)+\varepsilon\frac{\partial^2\vec{A}}{\partial t^2}+R\left[\vec{\nabla}\left(\vec{\nabla}\cdot\vec{A}\right)-\nabla^2\vec{A}\right]+\mathrm{LOT}=0 \quad (2.21)$$

The term LOT stands for Lower Order Terms (lower in differentiation). As is, these equations are still overdetermined since one can transform $A\to A'=A+df$ and arrive at the same set of equations. This is called a gauge transformation and represents an internal field symmetry in electromagnetism (distinct from Lorentz symmetry). There are an infinite number of potential equivalent descriptions of electromagnetism and, in principle, a gauge transform taking any description to any other description. One can "fix" a gauge by imposing a constraint on the potential. Three of the most common constraints are listed below.

$$\partial_t(\varepsilon\psi)+\vec{\nabla}\cdot\left(R\vec{A}\right)=0 \qquad \text{Lorentz} \quad (2.22)$$
$$\vec{\nabla}\cdot\vec{A}=0 \qquad \text{Coulomb} \quad (2.23)$$
$$\psi=0 \qquad \text{Temporal} \quad (2.24)$$

The form of the Lorentz gauge is taken from Deschamps [13]. For completeness and to document the result for future use, I present the full set of field equations for the 4-potential in the Lorentz gauge (Eq. 2.22) expanded in powers of the fields. Starting from Eqs. (2.18) and (2.19) each term is expanded.

$$\vec{\nabla}\varepsilon\cdot\vec{\nabla}\psi+\vec{\nabla}\varepsilon\cdot\frac{\partial\vec{A}}{\partial t}+\varepsilon\nabla^2\psi+\varepsilon\frac{\partial\vec{\nabla}\cdot\vec{A}}{\partial t}+\rho_f=0 \quad (2.25)$$

$$\varepsilon\frac{\partial^2\vec{A}}{\partial t^2}-R\nabla^2\vec{A}+\varepsilon\frac{\partial\vec{\nabla}\psi}{\partial t}+\frac{\partial\varepsilon}{\partial t}\vec{\nabla}\psi+\frac{\partial\varepsilon}{\partial t}\frac{\partial\vec{A}}{\partial t}+R\vec{\nabla}\left(\vec{\nabla}\cdot\vec{A}\right)+\vec{\nabla}R\times\left[\vec{\nabla}\times\vec{A}\right]-\vec{J}_f=0 \quad (2.26)$$

Focusing attention first on the equation for ψ, the gauge constraint provides the following expression for $\vec{\nabla}\cdot\vec{A}$.

$$\vec{\nabla}\cdot\vec{A}=-\frac{1}{R}\left(\frac{\partial\varepsilon\psi}{\partial t}+\vec{\nabla}R\cdot\vec{A}\right)$$

Explicitly differentiating in time, inserting the result into Eq. (2.25), and dividing through by ε leads to the following equation.

$$\nabla^2\psi + \frac{\vec{\nabla}\varepsilon}{\varepsilon}\cdot\vec{\nabla}\psi + \frac{\vec{\nabla}\varepsilon}{\varepsilon}\cdot\frac{\partial\vec{A}}{\partial t} + \frac{1}{R^2}\frac{\partial R}{\partial t}\left(\frac{\partial\varepsilon}{\partial t}\psi + \varepsilon\frac{\partial\psi}{\partial t} + \vec{\nabla}R\cdot\vec{A}\right) - \frac{1}{R}\left(\frac{\partial^2\varepsilon}{\partial t^2}\psi + \varepsilon\frac{\partial^2\psi}{\partial t^2} + 2\frac{\partial\varepsilon}{\partial t}\frac{\partial\psi}{\partial t} + \frac{\partial\left(\vec{\nabla}R\right)}{\partial t}\cdot\vec{A} + \vec{\nabla}R\cdot\frac{\partial\vec{A}}{\partial t}\right) + \frac{\rho_f}{\varepsilon} = 0$$

Rearranging terms in descending order of derivative and applying some calculus identities leads to the following final form of the equation for the scalar potential.

$$\nabla^2\psi - \frac{\varepsilon}{R}\frac{\partial^2\psi}{\partial t^2} + \frac{\vec{\nabla}\varepsilon}{\varepsilon}\cdot\vec{\nabla}\psi - \left(\frac{\partial}{\partial t}\left(\frac{\varepsilon}{R}\right) + \frac{1}{R}\frac{\partial\varepsilon}{\partial t}\right)\frac{\partial\psi}{\partial t} - \frac{\partial}{\partial t}\left(\frac{1}{R}\frac{\partial\varepsilon}{\partial t}\right)\psi + \left(\vec{\nabla}\ln\frac{\varepsilon}{R}\right)\cdot\frac{\partial\vec{A}}{\partial t} - \frac{\partial}{\partial t}\left(\frac{\vec{\nabla}R}{R}\right)\cdot\vec{A} = -\frac{\rho_f}{\varepsilon} \tag{2.27}$$

The form of Eq. (2.27) contains no terms with both $\vec{A}$ and ψ or their derivatives, and no mixed partials of either fields. The first two terms are the classic wave equation with an inhomogeneous wave speed, $c^{-2} = \varepsilon/R$. The next two terms contain first order derivatives of the field, ψ. Depending on the nature of the environment, these would act to produce dispersive effects and damping (or amplification) of the field. The next term is an effective mass term for the gauge field produced by time dependent fluctuations. The last two terms contain only the "vector" potential, $\vec{A}$, and could be treated as an effective source term. Several approximations are applicable to the study of long range propagation in the atmosphere. The first being that time dependent fluctuations will be very slow compared to the time scale required to detect echoes from objects in the environment. For all intents and purposes, one can treat the environment as being independent of time, with environmental profiles fixed over the time scale of a pulse or burst from a radar, and updated based on time of day or season. Eliminating terms containing time derivatives of the environmental factors leads to,

$$\nabla^2\psi - \frac{\varepsilon}{R}\frac{\partial^2\psi}{\partial t^2} + \frac{\vec{\nabla}\varepsilon}{\varepsilon}\cdot\vec{\nabla}\psi + \left(\vec{\nabla}\ln\frac{\varepsilon}{R}\right)\cdot\frac{\partial\vec{A}}{\partial t} = -\frac{\rho_f}{\varepsilon}$$

The second assumption that is often applied to this type of problem is that the magnetic properties of the environment are constant leaving only position dependent dielectric properties driving effects such as ducting. Assuming $R = \text{const.}$ results in the following reduced equation.

$$\nabla^2\psi - \frac{\varepsilon}{R}\frac{\partial^2\psi}{\partial t^2} + \frac{\vec{\nabla}\varepsilon}{\varepsilon}\cdot\left(\vec{\nabla}\psi + \frac{\partial\vec{A}}{\partial t}\right) = -\frac{\rho_f}{\varepsilon} \tag{2.28}$$

So far no "approximations" have been made. A common approximation applied to the environment is that the gradients terms are small compared to other terms, $\vec{\nabla}\varepsilon \approx 0$, allowing one to drop the gradient coupling from the equation. This is the only questionable approximation applied to the equations. It is often found in versions of the parabolic equation for the electric and magnetic fields as this allows one to completely decouple them leading to separate Helmholtz equations for each. Applying this assumption here eliminates terms containing $\vec{A}$ and its derivatives.

$$\nabla^2\psi - \frac{\varepsilon}{R}\frac{\partial^2\psi}{\partial t^2} \approx -\frac{\rho_f}{\varepsilon} \tag{2.29}$$

This form of the inhomogeneous wave equations in an inhomogeneous media is often assumed to be the starting point. One takes the equations for electrodynamics in a constant medium and simply inserts a position or time dependent function for all material parameters.

Next, consider field equation for $\vec{A}$ in same gauge. Using the gauge condition,

$$\frac{\partial\psi}{\partial t} = -\frac{1}{\varepsilon}\left(\frac{\partial\varepsilon}{\partial t}\psi + \vec{\nabla}\cdot\left(R\vec{A}\right)\right)$$

time derivate of ψ is eliminated in the equation for $\vec{A}$.

$$\varepsilon\frac{\partial^2\vec{A}}{\partial t^2} - R\nabla^2\vec{A} - \varepsilon\vec{\nabla}\left(\frac{1}{\varepsilon}\left(\frac{\partial\varepsilon}{\partial t}\psi + \vec{\nabla}\cdot\left(R\vec{A}\right)\right)\right) + \frac{\partial\varepsilon}{\partial t}\vec{\nabla}\psi + \frac{\partial\varepsilon}{\partial t}\frac{\partial\vec{A}}{\partial t} + R\vec{\nabla}\left(\vec{\nabla}\cdot\vec{A}\right) + \vec{\nabla}R\times\left[\vec{\nabla}\times\vec{A}\right] - \vec{J}_f = 0$$

Expanding the third term,

$$\begin{aligned}\varepsilon\vec{\nabla}\left(\frac{1}{\varepsilon}\frac{\partial\varepsilon}{\partial t}\psi + \frac{1}{\varepsilon}\vec{\nabla}\cdot\left(R\vec{A}\right)\right) &= \varepsilon\vec{\nabla}\left(\frac{1}{\varepsilon}\frac{\partial\varepsilon}{\partial t}\right)\psi + \frac{\partial\varepsilon}{\partial t}\vec{\nabla}\psi + \varepsilon\vec{\nabla}\left(\frac{1}{\varepsilon}\right)\vec{\nabla}\cdot\left(R\vec{A}\right) + \vec{\nabla}\left(\vec{\nabla}\cdot\left(R\vec{A}\right)\right)\\ &= \varepsilon\vec{\nabla}\left(\frac{1}{\varepsilon}\frac{\partial\varepsilon}{\partial t}\right)\psi + \frac{\partial\varepsilon}{\partial t}\vec{\nabla}\psi + \varepsilon\vec{\nabla}\left(\frac{1}{\varepsilon}\right)\vec{\nabla}\cdot\left(R\vec{A}\right) + \vec{\nabla}\left(\vec{\nabla}R\cdot\vec{A} + R\vec{\nabla}\cdot\vec{A}\right)\\ &= \varepsilon\vec{\nabla}\left(\frac{1}{\varepsilon}\frac{\partial\varepsilon}{\partial t}\right)\psi + \frac{\partial\varepsilon}{\partial t}\vec{\nabla}\psi + \varepsilon\vec{\nabla}\left(\frac{1}{\varepsilon}\right)\vec{\nabla}\cdot\left(R\vec{A}\right) + \vec{\nabla}\left(\vec{\nabla}R\cdot\vec{A}\right) + \vec{\nabla}R\vec{\nabla}\cdot\vec{A} + R\vec{\nabla}\left(\vec{\nabla}\cdot\vec{A}\right)\end{aligned}$$

The final general form of the vector potential equation is Eq. (2.30).

$$\begin{aligned}&\varepsilon\frac{\partial^2\vec{A}}{\partial t^2} - R\nabla^2\vec{A} + R\left(\frac{\vec{\nabla}\varepsilon}{\varepsilon} - \frac{\vec{\nabla}R}{R}\right)\vec{\nabla}\cdot\vec{A} - \left(\vec{\nabla}R\cdot\vec{\nabla}\right)\vec{A} + \frac{\partial\varepsilon}{\partial t}\frac{\partial\vec{A}}{\partial t} + \left(\frac{\vec{\nabla}\varepsilon}{\varepsilon}\vec{\nabla}R\cdot\vec{A} - \left(\vec{A}\cdot\vec{\nabla}\right)\vec{\nabla}R\right)\\ &\quad - \varepsilon\vec{\nabla}\left(\frac{1}{\varepsilon}\frac{\partial\varepsilon}{\partial t}\right)\psi - \vec{J}_f = 0\end{aligned} \tag{2.30}$$

Several vector identities have been used to reduce this equation to the above form. Assuming time independence of the medium eliminates the potential component ψ.

$$\varepsilon\frac{\partial^2\vec{A}}{\partial t^2} - R\nabla^2\vec{A} + R\left(\frac{\vec{\nabla}\varepsilon}{\varepsilon} - \frac{\vec{\nabla}R}{R}\right)\vec{\nabla}\cdot\vec{A} - \left(\vec{\nabla}R\cdot\vec{\nabla}\right)\vec{A} + \left(\frac{\vec{\nabla}\varepsilon}{\varepsilon}\vec{\nabla}R\cdot\vec{A} - \left(\vec{A}\cdot\vec{\nabla}\right)\vec{\nabla}R\right) - \vec{J}_f = 0$$

In practice the above equation could be solved for $\vec{A}$ and the result used as a source in the equivalent equation for ψ. Dividing through by R and rearranging terms,

$$\frac{\varepsilon}{R}\frac{\partial^2\vec{A}}{\partial t^2} - \nabla^2\vec{A} + \left(\frac{\vec{\nabla}\varepsilon}{\varepsilon} - \frac{\vec{\nabla}R}{R}\right)\vec{\nabla}\cdot\vec{A} - \frac{1}{R}\left(\vec{\nabla}R\cdot\vec{\nabla}\right)\vec{A} + \frac{1}{R}\left(\frac{\vec{\nabla}\varepsilon}{\varepsilon}\vec{\nabla}R\cdot\vec{A} - \left(\vec{A}\cdot\vec{\nabla}\right)\vec{\nabla}R\right) = \frac{\vec{J}_f}{R}$$

Assuming a magnetically constant medium reduces the above equation further,

$$\frac{\varepsilon}{R}\frac{\partial^2 \vec{A}}{\partial t^2} - \nabla^2 \vec{A} + \frac{\vec{\nabla}\varepsilon}{\varepsilon}\vec{\nabla}\cdot\vec{A} = \frac{\vec{J}_f}{R} \tag{2.31}$$

Finally, applying the approximation that the background gradients are small

$$\nabla^2 \vec{A} - \frac{\varepsilon}{R}\frac{\partial^2 \vec{A}}{\partial t^2} \approx -\frac{\vec{J}_f}{R} \tag{2.32}$$

Under the list of assumptions provided here each component of the 4-potential obeys the classic wave equation. A similar result holds for the electric and magnetic fields under the same set of assumptions. This leads to the classic Helmholtz equation and, after some additional assumptions the parabolic approximation. Assuming a time harmonic source,

$$\nabla^2 \vec{A} + \frac{\omega^2}{c^2}\vec{A} \approx -\frac{\vec{J}_f}{R}$$

$$\nabla^2 \psi + \frac{\omega^2}{c^2}\psi \approx -\frac{\rho_f}{\varepsilon}$$

This result should hold even in the presence of local wave speed that are slowly varying in spatial coordinates.

3. APPLICATION OF POLYNOMAL CHAOS TO MAXWELL

3.1 Expansion of the fields and parameters

The homogeneous polynomial chaos approach expresses each stochastic parameter and field in terms of a set of basis functions, which depend on an event space variable [24]. The basis is selected based on the known statistics of the input parameters so that a full description of the pdf is provided. The basis set is denoted by $\Phi^{(k)}(\theta)$, $k = 0, \cdots, \infty$, and θ denotes the event space parameter. These functions are orthonormal relative to a weighting function, $w(\theta)$, and can be chosen so that $w(\theta)$ represents the pdf that best suits the statistics of the input parameters, see Appendix D and references for details [25-40].

$$\left\langle \Phi^{(k)} \middle| \Phi^{(j)} \right\rangle \equiv \int \Phi^{(k)}\Phi^{(j)} w \, d\theta = \begin{cases} 1 & k = j \\ 0 & k \neq j \end{cases} \tag{3.1}$$

Equation (3.1) introduces the standard bra-ket notation (bra = ⟨ |, ket = | ⟩). Superscript indices in parenthesis map to distinct polynomial chaos basis elements, referred to in this report as "chaos modes". The notation is selected to avoid confusion with spatial indices, *e.g.* $E_k^{(i)}$ is the i^{th} chaos mode of the k^{th} component of the electric field 'vector'. The expansion is applied to Maxwell's equations where the electric modulus, $M = \varepsilon^{-1}$, and magnetic reluctance, $R = \mu^{-1}$, are the stochastic parameters that may depend on position and time, but otherwise describe an isotropic medium. The fields in the equations are the magnetic field vector, $\vec{B}$**,** and the electric displacement vector, $\vec{D}$. The expansion of all fields and parameters is provided below.

$$\vec{D} = \sum_{k=0}^{N} \vec{D}^{(k)} \Phi^{(k)}(\theta) \tag{3.2}$$

$$\vec{B} = \sum_{k=0}^{N} \vec{B}^{(k)} \Phi^{(k)}(\theta) \tag{3.3}$$

$$M = \sum_{k=0}^{N_e} M^{(k)} \Phi^{(k)}(\theta) \tag{3.4}$$

$$R = \sum_{k=0}^{N_m} R^{(k)} \Phi^{(k)}(\theta) \tag{3.5}$$

$$\vec{J} = \sum_{k=0}^{N_s} \vec{J}^{(k)} \Phi^{(k)}(\theta) \tag{3.6}$$

$$\rho = \sum_{k=0}^{N_s} \rho^{(k)} \Phi^{(k)}(\theta) \tag{3.7}$$

The summation limits are kept finite in anticipation of numerical implementation. For the output fields N is arbitrary, $N \to \infty$ formally but is determined by convergence tests in practice. The input parameters have limits N_e and N_m where the subscripts *e* and *m* refer to *electric* and *magnetic* parameters respectively, and the *s* in N_s stands for *source*. Typically, the input parameters can be described with just a few terms by selecting a basis and weighting function that closely resembles the statistics of the material.

3.2 Stochastic Maxwell's Equations (SME)

The primary goal is to investigate the nature of the characteristics and bicharacteristics associated with the SME. Anticipating the result is independent of source terms and constraints I focus first on "*stochasticizing*" the source free equations containing time derivative that lead to propagation, presenting the full set for completeness at the end of this section. Applying equations (3.2) – (3.7) to equations (2.3) – (2.4) lead, to equations (3.8) and (3.9).

$$\sum_{l=0}^{N} \Phi^{(l)} \frac{\partial \vec{B}^{(l)}}{\partial t} + \sum_{j,k=0}^{N,N_m} \Phi^{(k)} \Phi^{(j)} M^{(k)} \vec{\nabla} \times \vec{D}^{(j)} + \sum_{j,k=0}^{N,N_m} \Phi^{(k)} \Phi^{(j)} \vec{\nabla} M^{(k)} \times \vec{D}^{(j)} = 0 \tag{3.8}$$

$$\sum_{l=0}^{N} \Phi^{(l)} \frac{\partial \vec{D}^{(l)}}{\partial t} - \sum_{j,k=0}^{N,N_e} \Phi^{(k)} \Phi^{(j)} R^{(k)} \vec{\nabla} \times \vec{B}^{(j)} - \sum_{j,k=0}^{N,N_e} \Phi^{(k)} \Phi^{(j)} \vec{\nabla} R^{(k)} \times B^{(j)} = 0 \tag{3.9}$$

To generate a separate PDE for each chaos mode, the inner product of each equation with a sample basis element is formed, $\Phi^{(i)}$, *e.g.* $\langle \Phi^{(i)} | \text{Eq.}\,(3.8) \rangle$, *etc*. This process creates an infinite number of coupled equations, one for each chaos mode. The result appears in equations (3.10) and (3.11) where the following notation for the triple product is defined, $\langle \Phi^{(i)} | \Phi^{(k)} \Phi^{(j)} \rangle \equiv \varphi^{(ikj)}$.

$$\frac{\partial \vec{B}^{(i)}}{\partial t} + \sum_{i,j,k=0}^{N,N,N_e} \varphi^{(ikj)} M^{(k)} \vec{\nabla} \times \vec{D}^{(j)} + \sum_{i,j,k=0}^{N,N,N_e} \varphi^{(ikj)} \vec{\nabla} M^{(k)} \times \vec{D}^{(j)} = 0 \tag{3.10}$$

$$\frac{\partial \vec{D}^{(i)}}{\partial t} - \sum_{i,j,k=0}^{N,N,N_m} \varphi^{(ikj)} R^{(k)} \vec{\nabla} \times \vec{B}^{(j)} - \sum_{i,j,k=0}^{N,N,N_m} \varphi^{(ikj)} \vec{\nabla} R^{(k)} \times B^{(j)} = 0 \tag{3.11}$$

The parameter modes and the triple products are combined to form a set of chaos material property matrices.

$$M^{(ij)} \equiv \sum_{k=0}^{N_e} \varphi^{(ikj)} M^{(k)} \tag{3.12}$$

$$R^{(ij)} \equiv \sum_{k=0}^{N_m} \varphi^{(ikj)} R^{(k)} \tag{3.13}$$

The indices in these matrices map to chaos modes, not directions. The basis triple products, $\varphi^{(ikj)}$, are all constant (different for each pdf choice) and can be pulled in or out of derivative operators. Due to the permutation symmetry of $\varphi^{(ikj)}$, the material matrices are symmetric. The final form of the SME is,

$$\frac{\partial \vec{B}^{(i)}}{\partial t} + \sum_{i,j=0}^{N,N} M^{(ij)} \vec{\nabla} \times \vec{D}^{(j)} + \sum_{j,k=0}^{N,N} \vec{\nabla} M^{(ij)} \times \vec{D}^{(j)} = 0 \tag{3.14}$$

$$\frac{\partial \vec{D}^{(i)}}{\partial t} - \sum_{i,j=0}^{N,N} R^{(ij)} \vec{\nabla} \times \vec{B}^{(j)} - \sum_{i,j=0}^{N,N} \vec{\nabla} R^{(ij)} \times B^{(j)} = 0 \tag{3.15}$$

For completeness, the entire set of equations, expanded in the chaos basis, is presented for reference in later discussions. It is equations (3.14) and (3.15) that are used in the next section when the method of characteristics is applied.

$$\frac{\partial \vec{B}^{(i)}}{\partial t} + \sum_{i,j=0}^{N,N} \vec{\nabla} \times M^{(ij)} \vec{D}^{(j)} = 0 \tag{3.16}$$

$$-\frac{\partial \vec{D}^{(i)}}{\partial t} + \sum_{i,j=0}^{N,N} \vec{\nabla} \times R^{(ij)} \vec{B}^{(j)} = \vec{J}_f^{(i)} \tag{3.17}$$

$$\vec{\nabla} \cdot \vec{D}^{(i)} = \rho_f^{(i)} \tag{3.18}$$

$$\vec{\nabla} \cdot \vec{B}^{(i)} = 0 \tag{3.19}$$

3.3 Stochastic 2-forms and Maxwell's equations

Applying polynomial chaos to equations (2.11) and (2.13) provides an alternate description of SME. The full field tensor encompasses $\vec{E}$ and $\vec{B}$ in a single mathematical object. The vector and pseudo-vector natures of these fields are accounted for by the algebra of the 2-form. Expanding the field tensor in a chaos basis, $F = \sum \Phi^{(j)} F^{(j)}$, applying to equation (2.11), and projecting onto an independent basis, $\langle \Phi^{(i)} | dF \rangle$, leads to the following hierarchy of equations for the chaos modes of the tensor.

$$dF^{(i)} = 0 \tag{3.20}$$

To convert equation (2.13) requires expanding the source 4-vector and the Hodge operator. Hodge acts to map a basis *p*-form into a corresponding basis (*n*-*p*)-form. The use of 4D Hodge in chapter 2 was an abuse of notation. In the most general case, the potential equations developed in the last section of chapter 2 are needed.

At this point, the polynomial chaos is applied to the equations for the gauge potential, Eqs. (2.27) and (2.30). The most general form of these field equations is quite long. However, only the highest order derivative are needed to derive the characteristics.

$$\vec{A} = \sum_{k=0}^{N} \vec{A}^{(k)} \Phi^{(k)}(\theta) \tag{3.21}$$

$$\psi = \sum_{k=0}^{N} \psi^{(k)} \Phi^{(k)}(\theta) \tag{3.22}$$

Following the usual steps leads to the following set of stochastic equations.

$$\sum_{j=0}^{N} \left(M^{(ij)} \nabla^2 \psi^{(j)} - \mu^{(ij)} \frac{\partial^2 \psi^{(j)}}{\partial t^2} \right) + \text{LOT} = 0 \tag{3.23}$$

$$\sum_{j=0}^{N} \left(M^{(ij)} \nabla^2 \vec{A}^{(j)} - \mu^{(ij)} \frac{\partial^2 \vec{A}^{(j)}}{\partial t^2} \right) + \text{LOT} = 0 \tag{3.24}$$

Clearly, the chaos expansion should be applied to M and $R^{-1} = \mu$ in this case. There is freedom to move these factors around and, in theory, one could work directly with an expansion in c^2. These equations will be referred to as Stochastic Gauge Potential Equations (SGPE) in future sections.

3.4 Material parameters and the triple product integrals

In the previous section, a set of material matrices, $M^{(ij)}$ and $R^{(ij)}$, were introduced that are dependent on the expansion coefficients of each material model and the triple product of the specific basis used, see (3.12) and (3.13). Details regarding basis functions are in Appendix D. For most cases, the triple product $\varphi^{(ikj)}$ is sparse but the material matrices may not be. This section explores some of the properties or $M^{(ij)}$ and $R^{(ij)}$ that can be inferred from the triple product. The two factors that come into play are (1) the number of chaos modes used to describe the random material property and (2) the specific chaos basis used.

I analyze the structure of the material matrices and the induced wave speed matrix for simple cases. In general, theses matrices will be dense and symmetric, and some obvious patterns emerge with respect to developing the terms using chaos triple products. Most of the triple product matrices are very sparse due to selection rules for the triple integrals involved in their evaluation. Consider a special case as an example where both materials obey a uniform distribution.

$$R = \bar{R} + \Delta R \theta_1 \tag{3.25}$$

$$M = \bar{M} + \Delta M \theta_2 \tag{3.26}$$

In Eqs. (3.25) and (3.26), $\bar{X} = (X_2 + X_1)/2$, $\Delta X = (X_2 - X_1)/2$, where $X \in [X_1, X_2]$ and $\theta_i \sim U(-1, 1)$ for each i. This is the standard way to express a uniform random variable in terms of the standard uniform draw over the interval$[-1, 1]$. First, these must be expressed in terms of the normalized basis set, in this case Legendre polynomials. Using the information in Appendix D, it is straight forward to derive the following.

$$R = \sqrt{2}\bar{R}\hat{P}^{(0)} + \frac{\sqrt{2}}{\sqrt{3}}\Delta R\hat{P}^{(1)} \tag{3.27}$$

$$M = \sqrt{2}\bar{M}\hat{P}^{(0)} + \frac{\sqrt{2}}{\sqrt{3}}\Delta M\hat{P}^{(1)} \tag{3.28}$$

Strictly speaking, since there are two independent random variables, a direct product basis set is required to describe the SME. The appropriate functions are $\hat{\Phi}^{(s)}(\theta_1, \theta_2) = \hat{P}^{(n)}(\theta_1)\hat{P}^{(m)}(\theta_2)$ defined over the direct product space $[-1, 1] \times [-1, 1]$, and s is a unique index mapped to (n, m). The input fields, R and M, each depend on only one random variable and the other may be integrated out. The output fields, $\vec{E}^{(k)}$ and $\vec{B}^{(k)}$, must be expanded in terms of $\hat{\Phi}^{(s)}(\theta_1, \theta_2)$ to capture their full statistical behavior. Continuing with this example, the material matrices introduced in section 3.2 are constructed. Key to their construction are the selection rules for triple products of Legendre polynomials found in Appendix D. From these, it can be demonstrated that each will have a tri-diagonal form.

$$X^{(n,n)} = \sqrt{2}\bar{X}\langle\hat{P}^{(n)}\hat{P}^{(0)}\hat{P}^{(n)}\rangle = \bar{X}\langle\hat{P}^{(n)}\hat{P}^{(n)}\rangle = \bar{X} \tag{3.29}$$

$$X^{(n,n+1)} = \frac{\sqrt{2}}{\sqrt{3}}\Delta X\langle\hat{P}^{(n)}\hat{P}^{(1)}\hat{P}^{(n+1)}\rangle = \Delta X\frac{n+1}{\sqrt{2n+1}\sqrt{2n+3}} \tag{3.30}$$

Where X represents either variable, and $n = 0, \cdots, \infty$. In the limit of large n, the off-diagonal terms are approximated by $\Delta X/2$. The explicit form of the matrix is,

$$X = \begin{bmatrix} \bar{X} & \Delta X/\sqrt{3} & 0 & 0 & & \cdots & \\ \Delta X/\sqrt{3} & \bar{X} & 2\Delta X/\sqrt{15} & 0 & & \cdots & \\ 0 & 2\Delta X/\sqrt{15} & \bar{X} & 3\Delta X/\sqrt{35} & & \cdots & \\ 0 & 0 & 3\Delta X/\sqrt{35} & \bar{X} & & \cdots & \\ & & & & \ddots & \cdots & \\ & & & & \bar{X} & \Delta X/2 & 0 \\ \vdots & \vdots & \vdots & \vdots & \Delta X/2 & \bar{X} & \Delta X/2 \\ & & & & 0 & \Delta X/2 & \bar{X} \end{bmatrix} \tag{3.31}$$

To see how rapidly the off diagonal terms approach $\Delta X/2$, compare the first few coefficients, 0.5774, 0.5164, 0.5071, 0.5040, 0.5025, etc.

Next, consider the effect of adding a term to the expansion. This may arise in an attempt to describe the statistics of a more exotic variable, or one determined by an empirical data set where it is determined that Uniform is a good starting point for the expansion. In general, let's assume that one of the environment parameters is a function of a uniform RV, $X(\theta)$. A rather bad example (explained later) might be that permittivity has a uniform RV, $\varepsilon = \bar{\varepsilon} + \Delta\varepsilon\theta$. Then the inverse of this is, $M = (\bar{\varepsilon} + \Delta\varepsilon\theta)^{-1}$. A truncated

Taylor expansion could be used, but this would only be valid for small deviations. To build up the chaos expansion of this variable simply requires projecting M onto the chaos basis.

$$M = \sum \langle M(\theta) \big| \hat{P}^{(n)}(\theta) \rangle \hat{P}^{(n)}(\theta)$$

The above procedure is always valid but may not converge quickly. Back to the second order example.

$$X = X^{(0)}\hat{P}^{(0)} + X^{(1)}\hat{P}^{(1)} + X^{(2)}\hat{P}^{(2)}$$

The results in Appendix D is used to determine the allowed values of $\langle \hat{P}^{(m)}\hat{P}^{(2)}\hat{P}^{(n)}\rangle$. This term will be non-zero for all diagonal terms $n = m \geq 1$. The second order term will add to all diagonal, except $X^{(0,0)}$. For $n \neq m$, the selection rules imply that $m = n + 2$ are the only other allowed values. The second order term adds another off diagonal. The relevant triple products are,

$$\langle \hat{P}^{(n)}\hat{P}^{(2)}\hat{P}^{(n)}\rangle = \sqrt{\frac{5}{2}\frac{(n+1)n}{(2n+3)(2n-1)}}$$

$$\langle \hat{P}^{(n)}\hat{P}^{(2)}\hat{P}^{(n+2)}\rangle = \sqrt{\frac{5}{2}\frac{3}{2}}\frac{(n+2)(n+1)}{\sqrt{2n+1}\sqrt{2n+5}(2n+3)}$$

The limiting values as $n \to \infty$ are $\langle \hat{P}^{(n)}\hat{P}^{(2)}\hat{P}^{(n)}\rangle = \sqrt{5/2}(1/4)$ and $\langle \hat{P}^{(n)}\hat{P}^{(2)}\hat{P}^{(n+2)}\rangle = \sqrt{5/2}(3/8)$. The correction to Eq. (3.26) is provided in Eq. (3.32), with $X^{(2)} \equiv \sqrt{2/5}\nabla X$.

$$X = \begin{bmatrix} \bar{X} & \frac{\Delta X}{\sqrt{3}} & \frac{\nabla X}{\sqrt{5}} & 0 & & \cdots & \\ \frac{\Delta X}{\sqrt{3}} & \bar{X} + \frac{2\nabla X}{5} & \frac{2\Delta X}{\sqrt{15}} & \frac{6\nabla X}{5\sqrt{21}} & & \cdots & \\ \frac{\nabla X}{\sqrt{5}} & \frac{2\Delta X}{\sqrt{15}} & \bar{X} + \frac{2\nabla X}{7} & \frac{3\Delta X}{\sqrt{35}} & & \cdots & \\ 0 & \frac{6\nabla X}{5\sqrt{21}} & \frac{3\Delta X}{\sqrt{35}} & \bar{X} + \frac{4\nabla X}{15} & & \cdots & \\ & & & & \ddots & \cdots & \\ & & & & \bar{X} + \frac{\nabla X}{4} & \Delta X/2 & \frac{3\nabla X}{8} \\ \vdots & \vdots & \vdots & \vdots & \Delta X/2 & \bar{X} + \frac{\nabla X}{4} & \Delta X/2 \\ & & & & \frac{3\nabla X}{8} & \Delta X/2 & \bar{X} + \frac{\nabla X}{4} \end{bmatrix} \tag{3.32}$$

Now that the second example is complete, I'll explain why $M = (\bar{\varepsilon} + \Delta\varepsilon\theta)^{-1}$ is a silly idea. One has the freedom to develop the SME in any representation. If a system is presented with permittivity as the statistical input, $\varepsilon = \bar{\varepsilon} + \Delta\varepsilon\theta$, then the SME should be derived from Maxwell's equations with ε in the numerator. This ensures as few terms as possible are used in developing the inputs. The point of the above discussion was simply to inform the reader of how to approach developing SME in general cases where a parameter is a more complex functions of an RV. One can continue the process of deriving term by term additions to the material matrix based on adding more terms to the PCE but that doesn't reveal much. The nature of the terms will depend on the default pdf chosen for the RV and the selection rules may differ. The exercise was worth going through as a learning tool and to see how close a tri-diagonal Toeplitz form comes to approximating the first order uniform stochastic input, which will be useful in later sections.

4. CHARACTERISTICS OF SME

4.1 Method of characteristics applied to the SME

The method of characteristics is applied to the SME developed in the last chapter, equations (3.13) and (3.14). A detailed outline of the procedure is presented in Appendix A. Only the highest order linear derivatives contribute to the characteristic equation. For the SME, these would be the first two terms on the lhs of equations (3.13) and (3.14). The source terms do not contribute to the characteristics (hence their exclusion from the derivation. The third terms contain coupling of the fields to the material gradients through the factors $\vec{\nabla} M^{(ij)} \times \vec{D}^{(j)}$ and $\vec{\nabla} R^{(ij)} \times B^{(j)}$. Such terms can cause polarization rotation of an initial pulse as it propagates through the medium and may affect field amplitudes. These terms are often ignored (neglected) in parabolic approximations to Maxwell's equations, which causes a decoupling of the different independent polarizations in the parabolic equation (PE). No such approximation is required to develop the characteristic of the PDE system. To make equations simpler to read, the following notation is introduced, see Appendix B, where $p_0 = \partial_t \varphi$ and $\vec{p} = \vec{\nabla}\varphi$. This notation is chosen because of its similarity to momentum in mechanics. In fact, the derivatives of the characteristic surface defined by φ are related to the momentum along a ray path trajectory. Applying the method leads to the following form for the characteristic matrix.

$$\begin{bmatrix} p_0 \mathbf{1}_{3N} & \begin{pmatrix} M^{00}\vec{\boldsymbol{a}}\cdot\vec{p} & \cdots & M^{0N}\vec{\boldsymbol{a}}\cdot\vec{p} \\ \vdots & \ddots & \vdots \\ M^{N0}\vec{\boldsymbol{a}}\cdot\vec{p} & \cdots & M^{NN}\vec{\boldsymbol{a}}\cdot\vec{p} \end{pmatrix} \\ \begin{pmatrix} -R^{00}\vec{\boldsymbol{a}}\cdot\vec{p} & \cdots & -R^{0N}\vec{\boldsymbol{a}}\cdot\vec{p} \\ \vdots & \ddots & \vdots \\ -R^{N0}\vec{\boldsymbol{a}}\cdot\vec{p} & \cdots & -R^{NN}\vec{\boldsymbol{a}}\cdot\vec{p} \end{pmatrix} & p_0 \mathbf{1}_{3N} \end{bmatrix} \tag{4.1}$$

The diagonal blocks contain a single term, p_0, repeated once per equation, $\mathbf{1}_{3N}$ is shorthand for the identity matrix. There is no mixing of time derivatives of different chaos modes. The identity is of size $3N$ because each of the N chaos modes is a 3D vector. The off-diagonal blocks contain the factor $\vec{\boldsymbol{a}} \cdot \vec{p}$, a 3-by-3 matrix defined in Appendix A. Following the notation introduced in Appendix B, (B.10), $\mathbf{P} = \vec{\boldsymbol{a}} \cdot \vec{p}$. Finally, applying the definition of a direct product, equation (B.7), the characteristic matrix is written in block form,

$$\begin{bmatrix} \mathbf{1}_{3N} p_0 & \mathbf{M} \otimes \mathbf{P} \\ -\mathbf{R} \otimes \mathbf{P} & \mathbf{1}_{3N} p_0 \end{bmatrix} \tag{4.2}$$

The characteristics of the PDE are defined by those hyper-surfaces for which the determinant of equation (4.2) vanishes.

$$\det\begin{bmatrix} \mathbf{1}_{3N}p_0 & \mathbf{M}\otimes\mathbf{P} \\ -\mathbf{R}\otimes\mathbf{P} & \mathbf{1}_{3N}p_0 \end{bmatrix} = 0 \tag{4.3}$$

Several useful identities from Appendix B are applied to reduce this expression and eventually arrive at explicit forms for the characteristic surfaces of the SME. First note that the diagonal blocks commute with the off-diagonal blocks. This is trivial to demonstrate since the diagonal blocks are proportional to the identity, which commutes with everything.

$$\det\begin{bmatrix} \mathbf{1}_{3N}p_0 & \mathbf{M}\otimes\mathbf{P} \\ -\mathbf{R}\otimes\mathbf{P} & \mathbf{1}_{3N}p_0 \end{bmatrix} = \det\left(p_0^2\mathbf{1}_{3N} + (\mathbf{M}\otimes\mathbf{P})(\mathbf{R}\otimes\mathbf{P})\right)$$

The identity in equation (B.8) is used to rewrite the second term of the right hand side.

$$\det\left(p_0^2\mathbf{1}_{3N} + (\mathbf{M}\otimes\mathbf{P})(\mathbf{R}\otimes\mathbf{P})\right) = \det(p_0^2\mathbf{1}_{3N} + \mathbf{MR}\otimes\mathbf{P}^2) = \det(p_0^2\mathbf{1}_{3N} + \boldsymbol{c}^2\otimes\mathbf{P}^2)$$

The matrices $\mathbf{M}$ and $\mathbf{R}$, introduced in the previous chapter, each contain chaos modes describing the material constants. For Maxwell's equations in a homogeneous material the speed of light would be defined by $c^2 = MR = 1/(\varepsilon\mu)$. For notational convenience the squared wave speed matrix, $\boldsymbol{c}^2 = \mathbf{MR}$, is defined. The characteristic determinant in (4.3) is now in the following form.

$$\det(p_0^2\mathbf{1}_{3N} + \boldsymbol{c}^2\otimes\mathbf{P}^2) = 0 \tag{4.4}$$

To reduce this determinant further the direct product, $\boldsymbol{c}^2\otimes\mathbf{P}^2$, is expressed in terms of its eigenvalues and eigenvectors, *i.e.* $\boldsymbol{c}^2\otimes\mathbf{P}^2 = \boldsymbol{Q\Lambda Q^{-1}}$. Further noting that $\boldsymbol{QQ^{-1}} = \mathbf{1}_{3N}$, equation (4.4) is reduced to diagonal form.

$$\begin{gathered} \det(p_0^2\mathbf{1}_{3N} + \boldsymbol{c}^2\otimes\mathbf{P}^2) = \\ \det\left(p_0^2\boldsymbol{QQ^{-1}} + \boldsymbol{Q\Lambda Q^{-1}}\right) = \\ \det\left(\boldsymbol{Q}(p_0^2\mathbf{1}_{3N} + \boldsymbol{\Lambda})\boldsymbol{Q^{-1}}\right) = \\ \det\left((p_0^2\mathbf{1}_{3N} + \boldsymbol{\Lambda})\boldsymbol{Q^{-1}Q}\right) = \\ \det(p_0^2\mathbf{1}_{3N} + \boldsymbol{\Lambda}) = 0 \end{gathered}$$

All that is needed is an explicit expression for the eigenvalues in $\boldsymbol{\Lambda}$. Use of equations (B.9) and (B.11) accomplishes this. First, denote the eigenvalues of $\boldsymbol{c}^2$ by C_n^2. The matrix of eigenvalues can be expressed in terms of the C_n^2 and the eigenvalues of $\mathbf{P}^2$.

$$\boldsymbol{\Lambda} = \begin{pmatrix} \begin{pmatrix} 0 & & \\ & \ddots & \\ & & 0 \end{pmatrix}_{N\times N} & \mathbf{0} \\ \mathbf{0} & \begin{pmatrix} -p^2C_1^2 & & & & \\ & -p^2C_1^2 & & & \\ & & \ddots & & \\ & & & -p^2C_N^2 & \\ & & & & -p^2C_N^2 \end{pmatrix}_{2N\times 2N} \end{pmatrix}$$

This leads to the following diagonal form for the characteristic matrix.

$$p_0^2\mathbf{1}_{3N}+\boldsymbol{\Lambda}$$

$$=\begin{pmatrix} \begin{pmatrix} p_0^2 & & \\ & \ddots & \\ & & p_0^2 \end{pmatrix}_{N\times N} & \mathbf{0} \\ \mathbf{0} & \begin{pmatrix} p_0^2-p^2C_1^2 & & & & \\ & p_0^2-p^2C_1^2 & & & \\ & & \ddots & & \\ & & & p_0^2-p^2C_N^2 & \\ & & & & p_0^2-p^2C_N^2 \end{pmatrix}_{2N\times 2N} \end{pmatrix}$$

The determinant is now trivial, being the product of the diagonal terms.

$$\det(p_0^2\mathbf{1}_{3N}+\boldsymbol{c}^2\otimes\mathbf{P}^2)=p_0^{2N}(p_0^2-p^2C_1^2)^2\cdots(p_0^2-p^2C_N^2)^2=0 \qquad (4.5)$$

If one started with the alternate representation mentioned in chapter 2, the form of the characteristics would be the same but with factors $C_n^{-2}p_0^2-p^2$.

4.2 Method of characteristics applied to the SGPE

Taking the same approach as the previous section and referring to Appendix A for details on second order equations, the characteristic matrix for Eqs. (3.23) and (3.24) is derived.

$$[\mathbf{M}p^2-\boldsymbol{\mu}p_0^2] \qquad (4.6)$$

This system leads to a much simpler characteristic matrix since all second-order derivatives are scalar in nature (*i.e.* no curl operations, only the Laplacian enters in the equations). Taking the determinant, the only linear algebra trick needed is pulling out one of the two material operators form the sum.

$$\det[\mathbf{M}p^2-\boldsymbol{\mu}p_0^2]=\det\boldsymbol{\mu}\det[\mathbf{M}\boldsymbol{\mu}^{-1}p^2-\mathbf{1}_{\boldsymbol{N}}p_0^2]=\det\boldsymbol{\mu}\det\left[\tilde{\boldsymbol{c}}^{\mathbf{2}}p^2-\mathbf{1}_{\boldsymbol{N}}p_0^2\right] \qquad (4.7)$$

The squared wave speed matrix, $\tilde{\boldsymbol{c}}^{\mathbf{2}}=\mathbf{M}\boldsymbol{\mu}^{-1}$, is defined and will not generally be the same as the $\boldsymbol{c}^{\mathbf{2}}$ defined in the previous section. Applying the same steps to the last factor on the right of Eq. (4.7) gives a similar result as before.

$$\det\left[\tilde{\boldsymbol{c}}^{\mathbf{2}}p^2-\mathbf{1}_{\boldsymbol{N}}p_0^2\right]=\prod_{n=0}^{N}\left(\tilde{C}_n^2p^2-p_0^2\right)=0 \qquad (4.8)$$

The chaos modes of the gauge potential are described by a set of independent characteristics each defining a light cone structure. Referring to appendix A, the characteristic matrix can vary considerably depending on the gauge selected. For the Coulomb gauge an entire dimension is eliminated, and the resulting matrix is dense with mixed terms in each entry. The characteristic matrix is diagonal in the Lorentz gauge making it very easy to work with.

4.3 Analysis of the eigenvalue spectrum

To get an example of what the eigenvalue spectrum might look like consider the simple example of section 3.4. Multiplying two tridiagonal matrices produces a penta-diagonal matrix. In general, the result will not be symmetric even if the original matrices are. In this special case where both parameters obey the same statistics, the product does produce a symmetric form, only the upper 5×5 is shown here, with $\bar{R}\bar{M} \equiv a$, $\Delta R \Delta M \equiv b$, and $\bar{R}\Delta M + \bar{M}\Delta R \equiv c$.

$$\boldsymbol{c^2} = \begin{bmatrix} a + \frac{b}{3} & \frac{c}{\sqrt{3}} & \frac{2b}{3\sqrt{5}} & 0 & 0 \\ \frac{c}{\sqrt{3}} & a + \frac{3b}{5} & \frac{2c}{\sqrt{15}} & \frac{6b}{5\sqrt{21}} & 0 \\ \frac{2b}{3\sqrt{5}} & \frac{2c}{\sqrt{15}} & a + \frac{11b}{21} & \frac{3c}{\sqrt{35}} & \frac{4b}{\sqrt{7}\sqrt{35}} \\ 0 & \frac{6b}{5\sqrt{21}} & \frac{3c}{\sqrt{35}} & a + \frac{39b}{77} & \frac{5c}{3\sqrt{11}} \\ 0 & 0 & \frac{4b}{\sqrt{7}\sqrt{35}} & \frac{5c}{3\sqrt{11}} & a + \frac{59b}{117} \end{bmatrix} \tag{4.6}$$

The reason for the serendipitous symmetry is due to each matrix being derived from the same expansion. If, for example, one variable was uniform and the other normal, $\boldsymbol{c^2}$ would not have been symmetric. Now assume that the magnetic properties of the medium are constant and the only RV is M given by a uniform distribution. In this case,

$$\boldsymbol{c^2} = R^{(0)} \begin{bmatrix} \bar{M} & \Delta M/\sqrt{3} & 0 & 0 & & \cdots & \\ \Delta M/\sqrt{3} & \bar{M} & 2\Delta M/\sqrt{15} & 0 & & \cdots & \\ 0 & 2\Delta M/\sqrt{15} & \bar{M} & 3\Delta M/\sqrt{35} & & \cdots & \\ 0 & 0 & 3\Delta M/\sqrt{35} & \bar{M} & & \cdots & \\ & & & & \ddots & \cdots & \\ & & & & \bar{M} & \Delta M/2 & 0 \\ \vdots & \vdots & \vdots & \vdots & \Delta M/2 & \bar{M} & \Delta M/2 \\ & & & & 0 & \Delta M/2 & \bar{M} \end{bmatrix}$$

For illustrative purposes, assume that the above matrix is approximated by a Toeplitz form. Considering the discussion in section 3.4, the off-diagonal coefficients could be approximated by the average value of the Legendre triple product or simply by the asymptotic value $\Delta M/2$. Choosing the latter,

$$\boldsymbol{c^2} \approx R^{(0)} \begin{bmatrix} \bar{M} & \Delta M/2 & 0 & \\ \Delta M/2 & \bar{M} & \Delta M/2 & \\ 0 & \Delta M/2 & \bar{M} & \\ & & & \ddots \end{bmatrix}$$

For which well-known exact formula for the eigenvalues and eigenvectors can be used.

$$C_n^2 = R^{(0)} \left(\bar{M} + \Delta M \cos \frac{n\pi}{N+1} \right) \tag{4.7}$$

$$\hat{\mathrm{v}}_n(k) = A_n \sin\left(\frac{nk\pi}{N+1}\right) \tag{4.8}$$

The value N is the size of the truncated matrix, $n = 1, 2, \cdots, N$, and $k = 1, 2, \cdots, N$ labels the component of the eigenvector. The constant A_n is a normalization factor. If both matrices are approximated by a Toeplitz matrix, the product becomes simpler than Eq. (4.6).

$$\boldsymbol{c^2} \approx \begin{bmatrix} a+\frac{b}{4} & \frac{c}{2} & \frac{b}{4} & 0 & 0 \\ \frac{c}{2} & a+\frac{b}{2} & \frac{c}{2} & \frac{b}{4} & 0 \\ \frac{b}{4} & \frac{c}{2} & a+\frac{b}{2} & \frac{c}{2} & \frac{b}{4} \\ 0 & \frac{b}{4} & \frac{c}{2} & a+\frac{b}{2} & \frac{c}{2} \\ 0 & 0 & \frac{b}{4} & \frac{c}{2} & a+\frac{b}{2} \end{bmatrix}$$

Only the first element (upper left) prevents this from being a penta-diagonal Toeplitz matrix. Simple formulas for larger Toeplitz matrices are not as prevalent as for the tri-diagonal form. This section concludes with an explicit comparison of the numerical eigenvalues and eigenvectors to the approximate Toeplitz solution for a medium described by a uniform distributed M and constant R.

Consider a material with relative permittivity $\varepsilon = \bar{\varepsilon} + \Delta\varepsilon\theta$ with θ a standard uniform variable, and limits on $[1.5, 1.8]$. From these limits, $\bar{\varepsilon} = 1.65$ and $\Delta\varepsilon = 0.15$. Comparisons are shown between "exact" and "approximate" values. The "exact" value is determined by applying Matlab eigenvalue function ***eig***() to Eq. (3.16) while the "approximate" value uses Eq. (4.7) for the Toeplitz matrix form using $\Delta\varepsilon/2$ for all off diagonal values. Table 1 compares values for N = 2, just 2 modes used in describing the full system. One sees that the values compare well, differing in the 3rd significant figure. Table 2 provides the same comparison for N = 5. As the size of the matrix increases, the match gets better. Figures 1 and 2 are eigenvalue comparisons for N = 10 and N = 100 respectively. In Figure 2, the approximate values are plotted for every 10th eigenvalue index starting from 1.

Table 1 – Exact vs approximate eigenvalues for N = 2

Eigenvalues for N = 2		
n	"Exact"	Approximate
1	1.7366	1.7250
2	1.5634	1.5750

Table 2 – Exact vs approximate eigenvalues for N = 5

Eigenvalues for N = 5		
n	"Exact"	Approximate
1	1.7859	1.7799
2	1.7308	1.7250
3	1.6500	1.6500
4	1.5692	1.5750
5	1.5141	1.5201

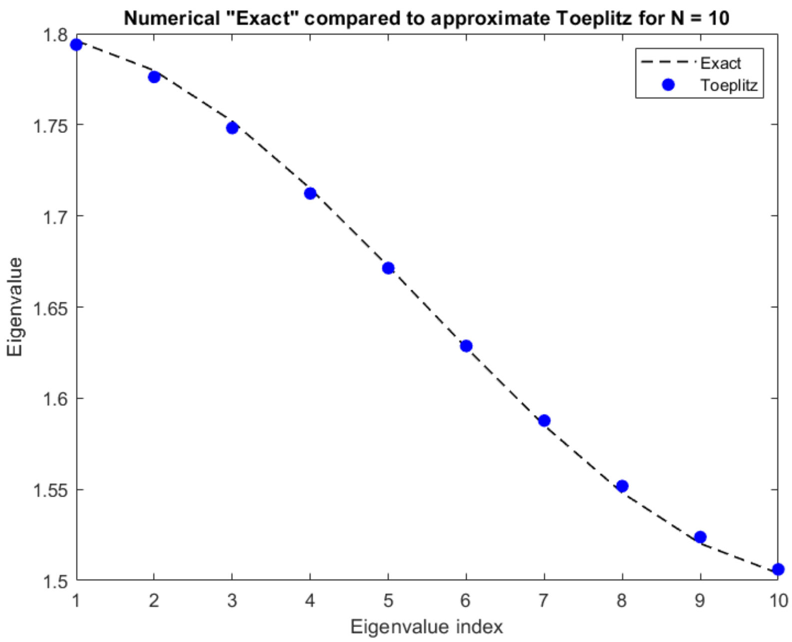

Figure 1 – Exact vs Approximate eigenvalues for N = 10.

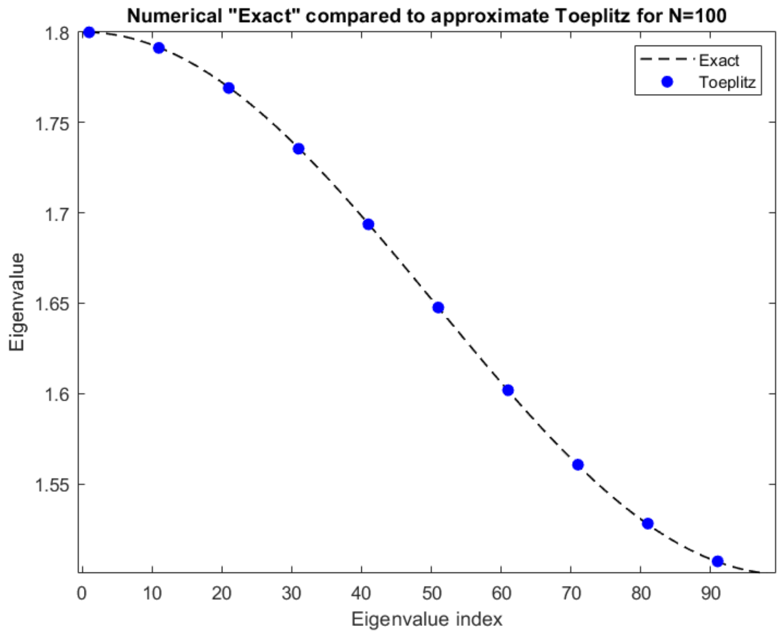

Figure 2 – Exact vs Approximate eigenvalues for N = 100.

Finally, table 3 provides the maximum percent difference between exact (E) and approximate (T, for Toeplitz) for N = 2, 5, 10, 100. The trend to better estimates of the eigenvalues is apparent.

Table 3 – Maximum % difference in eigenvalues (Exact vs Approximate)

Maximum % difference	
N	max(|E-T|/E)*100
2	0.74
5	0.40
10	0.24
100	0.027

Since this example used relative permittivity, the eigenvalues correspond to $1/c^2$ with an appropriate scale factor included. The corresponding wave speed in units of c_0, the speed of light in vacuum, for the N = 5 case are given below in table 4.

Table 4 – Wave speeds associated with each eigenvalue of the permittivity matrix

Wave speed for N = 5 permittivity eigenvalues		
N	ε	c/c_0
1	1.7859	0.7483
2	1.7308	0.7601
3	1.6500	0.7785
4	1.5692	0.7983
5	1.5141	0.8127

4.4 Light cones and SME geometry

The case $N = 1$ corresponds to the characteristic for Maxwell's original equations, $p_0^2(p_0^2 - p^2c^2)^2 = 0$. The characteristic $p_0^2 - p^2c^2 = 0$ defines the light cone introduced by Einstein in the theory of relativity. In terms of the characteristic surface, φ, the equation reads as $(\partial_t\varphi)^2 = c^2\left|\vec{\nabla}\varphi\right|^2$. Each factor in equation (4.5) defines a partial Hamiltonian, the variation of which produces a ray equation, or more generally, the bicharacteristic paths in space-time that are everywhere orthogonal (in a covariant sense) to the characteristic surfaces. Following the same reasoning as classical treatments of Maxwell's equations there are an infinite number of light cone structures for the SME, one for each eigenvalue of the wave speed matrix, $p_0^2 - p^2C_n^2 = 0$. The characteristic equation is still valid when the material parameters are functions of position and time even through the material gradients do not enter the picture.

At this point, I introduce the interpretation of bicharacteristics as geodesics of an effective manifold with an environment induced metric tensor. Appendix C provides a quick tutorial on the basic vocabulary used in this section. The components of the 3D vector $\vec{p}$ and the scalar p_0 are combined into a covariant 4-vector, $p_\mu = [p_0 \quad \vec{p}]^T$, with $\mu = 0,1,2,3$. The $\mu = 0$ component corresponds to the time direction and the others to spatial direction. The characteristic is identified with the magnitude of this 4-vector relative to a non-Euclidian metric tensor.

$$p_0^2 - p^2c^2 = [p_0 \quad \vec{p}]\begin{bmatrix}1 & \mathbf{0} \\ \mathbf{0} & -c^2\mathbf{1}_3\end{bmatrix}\begin{bmatrix}p_0 \\ \vec{p}\end{bmatrix} \tag{4.9}$$

The matrix is identified with the components of the contravariant metric tensor.

$$g^{\mu\nu} = \begin{bmatrix}1 & \mathbf{0} \\ \mathbf{0} & -c^2\mathbf{1}_3\end{bmatrix} \tag{4.10}$$

Using equation (4.10) the characteristic condition is expressed as a covariant inner product relative to $g^{\mu\nu}$.

$$g^{\mu\nu}p_\mu p_\nu = 0 \tag{4.11}$$

Equation (4.11) states that the 4-gradient of the characteristic surface is a vector of zero magnitude at every point in space-time. The covariant metric is defined by the condition that it be the inverse of the contravariant metric.

$$g^{\mu\nu}g_{\nu\alpha} = \delta_\alpha^\mu \tag{4.12}$$

From the matrix form of $g^{\mu\nu}$, the components of $g_{\mu\nu}$ can be immediately determined.

$$g_{\mu\nu} = \begin{bmatrix} 1 & \mathbf{0} \\ \mathbf{0} & -c^{-2}\mathbf{1}_3 \end{bmatrix} \tag{4.13}$$

Using $g^{\mu\nu}$ a contravariant version of p_ν is defined in terms of local coordinate differentials.

$$\frac{dx^\mu}{d\lambda} = p^\mu = g^{\mu\nu}p_\nu \tag{4.14}$$

The covariant 4-vector, p_ν, are components of the 4D gradient of the wavefront and the contravariant 4-vector components of the 4D velocity of a ray path. In terms of these new variables, the characteristic equation becomes equation (4.15) below.

$$g_{\mu\nu}\frac{dx^\mu}{d\lambda}\frac{dx^\nu}{d\lambda} = 0 \tag{4.15}$$

The parameter λ (called an affine parameter) labels points along a 4-trajectory, $x^\mu(\lambda)$. Equation (4.15) also implies the infinitesimal 4-length, dS, along the ray path vanishes.

$$dS^2 \equiv g_{\mu\nu}dx^\mu dx^\nu = 0 \tag{4.16}$$

One can easily confirm that the basic relation between 3-length and time from optics is implied by equation (4.16).

The discussion above focused on Maxwell's classical equations and a single wave speed. The results apply to each factor in equation (4.5). The SME defines an infinite number of characteristics, each with an effective metric defined by the eigenvalues, C_n^2, of the wave speed matrix. Each propagates independently of the others and all contribute to building the total stochastic field. This will be elaborated on in chapter 5. The reader may be thinking, quite naturally, why I didn't just define ray paths, Fermat times and metric strictures in the beginning then apply them to the problem. If the goal was to teach a tutorial on differential geometry or ray theory, that might be the natural progression of topics. Referring to the comments in the introduction, the main point is to demonstrate that Maxwell's equations predicts the features commonly found in optics and that these structures naturally emerge by applying the method of characteristics to a PDE. In fact, this is precisely how such topics are introduced in Courant & Hilbert and many other texts on the subject. From both a mathematical and physical point of view, ray paths, travel times, and even differential geometry are all features of the PDE to be discovered through this process rather than imposed on it *a priori*. In fact, this familiar structure was not guaranteed to emerge for the SME, and imposing it could have caused inconsistent results. In chapter 6, I consider the effect of making such assumptions without justification on the resulting stochastic ray equation (SRE). Chapter 4 with a section on the classic ray equation and the rays of the SME.

4.5 Ray path equations in 4-dimensional space-time

Combining the results of the previous section and Appendix C, the covariant space-time equations for the bicharacteristic curves is determined.

$$\frac{d^2t}{d\lambda^2}+\frac{1}{2}\frac{\partial C_n^{-2}}{\partial t}\left|\frac{d\vec{x}}{d\lambda}\right|^2=0 \tag{4.17}$$

$$\frac{d^2\vec{x}}{d\lambda^2}+\frac{C_n^2}{2}\vec{\nabla}C_n^{-2}\left|\frac{d\vec{x}}{d\lambda}\right|^2-C_n^2\left(\vec{\nabla}C_n^{-2}\cdot\frac{d\vec{x}}{d\lambda}\right)\frac{d\vec{x}}{d\lambda}+\frac{C_n^2}{2}\frac{\partial C_n^{-2}}{\partial t}\frac{dt}{d\lambda}\frac{d\vec{x}}{d\lambda}=0 \tag{4.18}$$

Equations (4.17) and (4.18) are the result of brute force application of C.4 using (4.10) and (4.13). In addition to the geodesic equation, the original characteristic imposes the null constraint, (4.15), along the path. The bicharacteristics are null geodesics. This feature is true of any hyperbolic PDE, including acoustics and electromagnetism, and is often overlooked. Null paths in space-time have a symmetry no other path possesses called conformal symmetry. The metric can be multiplied by any positive function, along with a suitable redefinition of $d\lambda$, and the geometry of these paths remains the same. A complete set of conformal transformations are found in reference [46]. For example, one can use the conformally equivalent metric and its inverse (modulo a constant factor to account for units).

$$\tilde{g}_{\mu\nu}=\begin{bmatrix}c^2 & \mathbf{0}\\ \mathbf{0} & -\mathbf{1}_3\end{bmatrix} \tag{4.19}$$

Equation 4.19 results in the following geodesic equations.

$$\frac{d^2t}{d\lambda^2}+\frac{1}{2}\frac{1}{C_n^2}\frac{\partial C_n^2}{\partial t}\left(\frac{dt}{d\lambda}\right)^2+\frac{1}{2}\frac{1}{C_n^2}\left(\vec{\nabla}C_n^2\cdot\frac{d\vec{x}}{d\lambda}\right)\frac{dt}{d\lambda}=0 \tag{4.20}$$

$$\frac{d^2\vec{x}}{d\lambda^2}-\frac{1}{2}\vec{\nabla}C_n^2\left(\frac{dt}{d\lambda}\right)^2=0 \tag{4.21}$$

The null condition can be used to further reduce complexity in some of the terms in either pair of equations 4.17 and 4.18, or 4.20 and 4.21. In numerical implementations the null condition can be used to regulate step size ensuring energy conservation along the path based on a threshold. Readers may not be familiar with ray theory expressed in terms of geodesics. To make contact with familiar forms I present the equation for ray paths parameterized by time along the ray.

$$\frac{d^2\vec{x}}{dt^2}=-c\vec{\nabla}c+2\frac{1}{c}\frac{d\vec{x}}{dt}\frac{d\vec{x}}{dt}\cdot\vec{\nabla}c+\frac{d\vec{x}}{dt}\frac{1}{c}\frac{\partial c}{\partial t} \tag{4.22}$$

Even more common is the following expression for 3D arc-length parameterized ray paths in the presence of a position dependent local wave speed [47].

$$\frac{d}{ds}\left(\frac{1}{c}\frac{d\vec{x}}{ds}\right) = \vec{\nabla}\frac{1}{c} \tag{4.23}$$

Changing parameter to $d\sigma = cds$ leads to the “Newton” representation of ray theory, so called because the ray path represents Newton’s second law with a conservative force.

$$\frac{d^2\vec{x}}{d\sigma^2} = \frac{1}{c}\vec{\nabla}\frac{1}{c} \tag{4.24}$$

Equations (4.22) through (4.24) can all be derived from the geodesic equation making it, in my opinion, the best format for discussing ray theory and ray trace techniques.

4.6 Position dependent materials

Position dependent material properties are common, occurring naturally, *e.g.* ducting caused by height varying refractive index, or by man-made processes, *e.g.* refractive waveguides created by layered media. Regardless, the result can be expressed by $\varepsilon(\vec{x})$ and $\mu(\vec{x})$ or $M(\vec{x})$ and $R(\vec{x})$. The ray paths are only sensitive to the combination $c(\vec{x}) = \sqrt{M(\vec{x})R(\vec{x})}$. The polynomial chaos approach is valid in the presence of position dependent parameters. This is explored in the following subsection.

4.6.1 Uncertain parameters in material definitions

A chaos expansion for either $M(\vec{x})$, $R(\vec{x})$, or both induces a similar expansion in $c(\vec{x})$. This happens, for example, when the coefficients in the description of the environment are uncertain. An example is provided in Eq. 4.25. The relative permittivity is a constant with a height dependent quadratic change, height being measured by z. A quadratic function is selected to ensure that the effective wave speed never becomes superluminal. This model has three free parameters. The first is a constant relative permittivity, ε_0, (not the permittivity of free space). The second, δ_2, measures the strength of quadratic change and is assumed here to be positive. The third free parameter, z_0, sets the height at which the minimum value occurs.

$$\varepsilon = \varepsilon_0 + \delta_2(z - z_0)^2 \tag{4.25}$$

As a second example consider adding a Gaussian bump to the local permittivity.

$$\varepsilon = \varepsilon_0 + \delta_2 \exp(-(z - z_0)^2/2\sigma^2) \tag{4.26}$$

Assume that either model accurately describes a type of refractive effect where the three free parameters contain come uncertainty, are described by random variables, *e.g.* $\varepsilon_0 = \bar{\varepsilon} + \Delta\varepsilon\theta_1$, $\delta_2 = \bar{\delta} + \Delta\delta\theta_2$, $z_0 = \bar{z} + \Delta z\theta_3$, and $\sigma = \bar{\sigma} + \Delta\sigma\theta_4$ where $\theta_i \sim U(-1, 1)$ for all I, and each variable is bound within limits $[X_{min}, X_{Max}]$. For the quadratic example the correct polynomial chaos basis would be a triple tensor product, $\hat{\Phi}^{(s)}(\vec{\theta}) = \hat{P}^{(l)}(\theta_1)\hat{P}^{(m)}(\theta_2)\hat{P}^{(n)}(\theta_3)$, where s is a unique index that maps to the combination

(l, m, n). Figures 3 through 6 show example permittivity and wave speed profiles for 5 random draws for both examples.

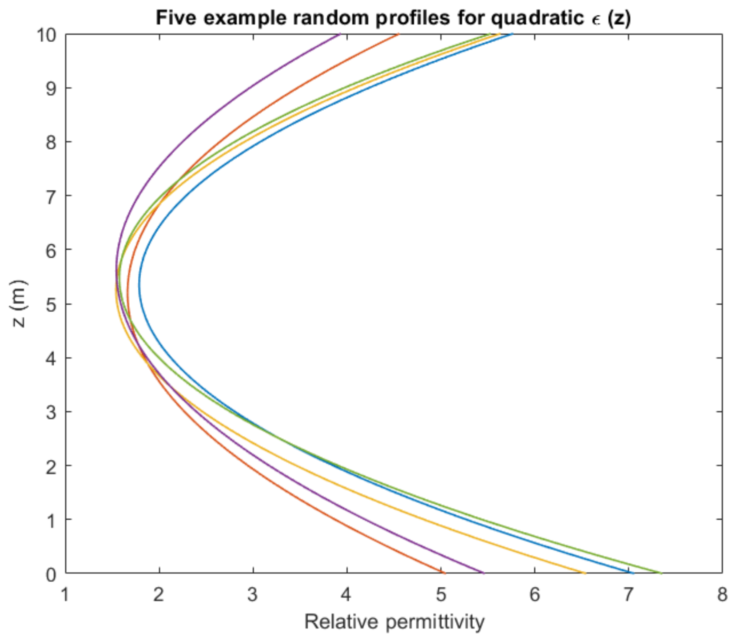

Figure 3 – Example permittivity functions generated from Eq. (4.25)

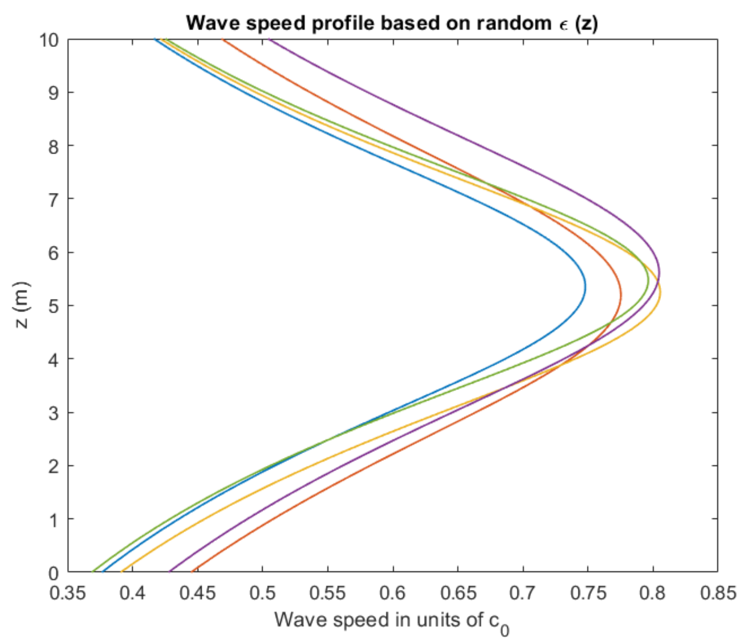

Figure 4 – Example wave speed profiles generated from the permittivity in Figure 3.

The quadratic variation in permittivity causes an increase with increasing $|z|$, which generates a wave speed profile that eventually tends to zero as $|z| \to \infty$. There is a max value at $z = z_0$. Ray paths will diverge and tend to bend toward $|z| \to \infty$. In general, waves tend to gravitate towards regions of minimum wave speed. The zero speed may seem unphysical but it occurs at infinity. The profile can be used in a finite region between boundaries with no issues.

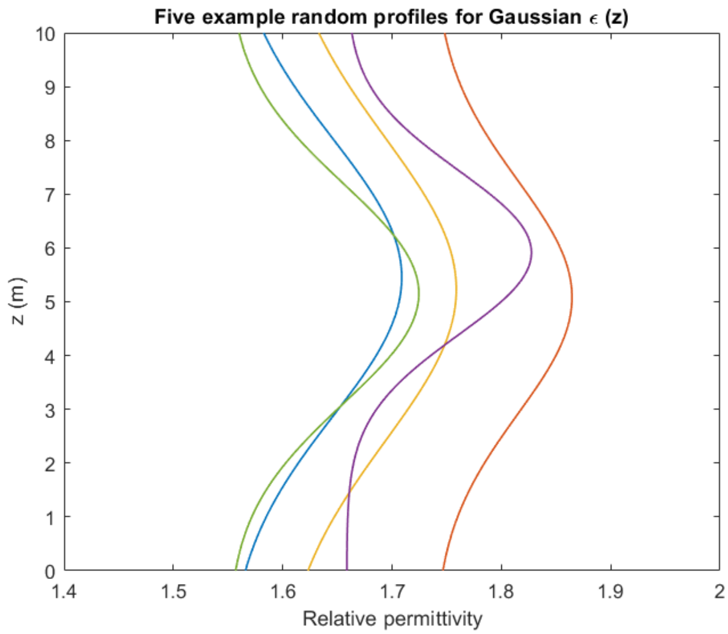

Figure 5 - Example permittivity functions generated from Eq. (4.26)

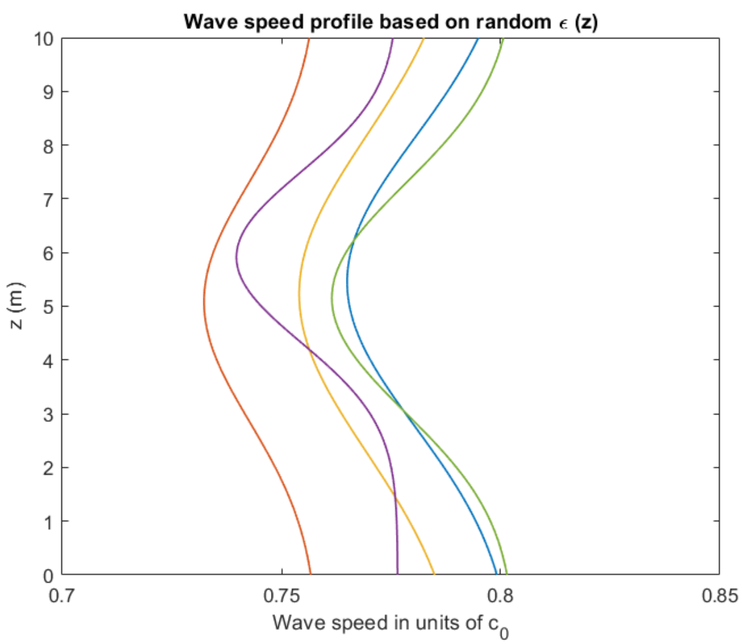

Figure 6 - Example wave speed profiles generated from the permittivity in Figure 5

The Gaussian bump produces a local maximum in the permittivity which generates a local minimum in the wave speed. This will create a duct, trapping ray paths with shallow launch angles. These rays will oscillate about the waveguide axis, $z = z_0$. Rays with steeper launch angles may propagate to infinity without a turning point. The random features of the wave speed profile will drive random results in the ray paths.

Consider a simpler the example with the following RV.

$$\varepsilon = \varepsilon_0 + \delta_2 f(z) = \left(\varepsilon_0 + \bar{\delta} f(z)\right) + \Delta\delta f(z)\theta \tag{4.27}$$

The only RV is the strength parameter $\delta_2 = \bar{\delta} + \Delta\delta\theta$, uniformly distributed with $\delta_2 \geq 0$, and $f(z) \geq 0$. This covers a wide class of refractive profiles each with a random strength. The second equality in Eq. (4.27) separates out the zeroth and first order polynomial chaos modes, and can be mapped to the previous examples, $\bar{\varepsilon}(z) = \varepsilon_0 + \bar{\delta} f(z)$ and $\Delta\varepsilon(z) = \Delta\delta f(z)$. Using this definition, every result previously discussed can be applied to this class of problems. In particular, the material matrix developed using the triple integral over Legendre polynomials will be identical to Eq. (3.31) with $\bar{\varepsilon}$ and $\Delta\varepsilon$ replaced by appropriate functions of position. Using the Toeplitz eigenvalues as an approximation, leads to the following spectrum for the wave speed.

$$C_n(z) = \frac{1}{\sqrt{\varepsilon_0 + \left(\bar{\delta} + \Delta\delta \cos\left(\frac{n\pi}{N+1}\right)\right) f(z)}} \tag{4.28}$$

If a uniform inverse permittivity was used, $M(\vec{x})$, the same analysis would lead to the following wave speed spectrum, where δ is interpreted as a variation in M.

$$C_n(z) = \sqrt{M_0 + \left(\bar{\delta} + \Delta\delta \cos\left(\frac{n\pi}{N+1}\right)\right) f(z)} \tag{4.29}$$

The "eigen" wave speed profiles for a Gaussian function are provided in figure 7.

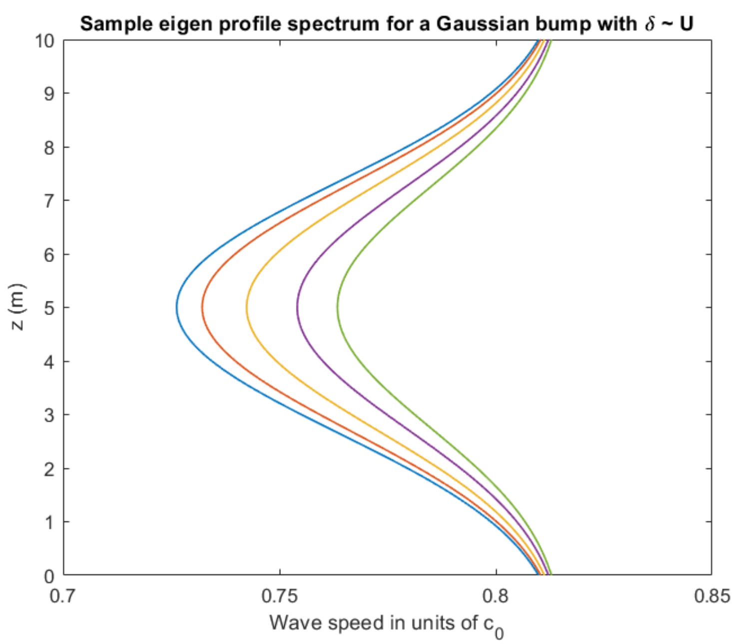

Figure 7 – Sample wave speed profiles generated by the eigenvalues of Eq. (4.29)

5. INTERPRETATION AND EXAMPLE

5.1 Physical interpretation of the characteristics of SME

In ordinary electromagnetism, the ray path or bicharacteristics represent paths of propagation. Standard derivations relate these to paths along which the field intensity is conserved. More generally, the surface of initial data describing the fields in the PDE are pushed forward to a new surface along these paths. The treatment of the SME led to an infinite number of decoupled ray paths, one for each eigenvalue of the square wave speed matrix. Even though the chaos modes are coupled by the SME, the ray paths seem to be uncoupled. Each defined some type of energy propagation path in space and all contribute to the total field at any given point in space-time. This is illustrated in Figure 8. The only thing that can be measured is some ensemble average or the m^{th} moment of the field at a given point in space-time so whatever these paths represent is not directly observable or measureable, but the ensemble average produces the observed mean field.

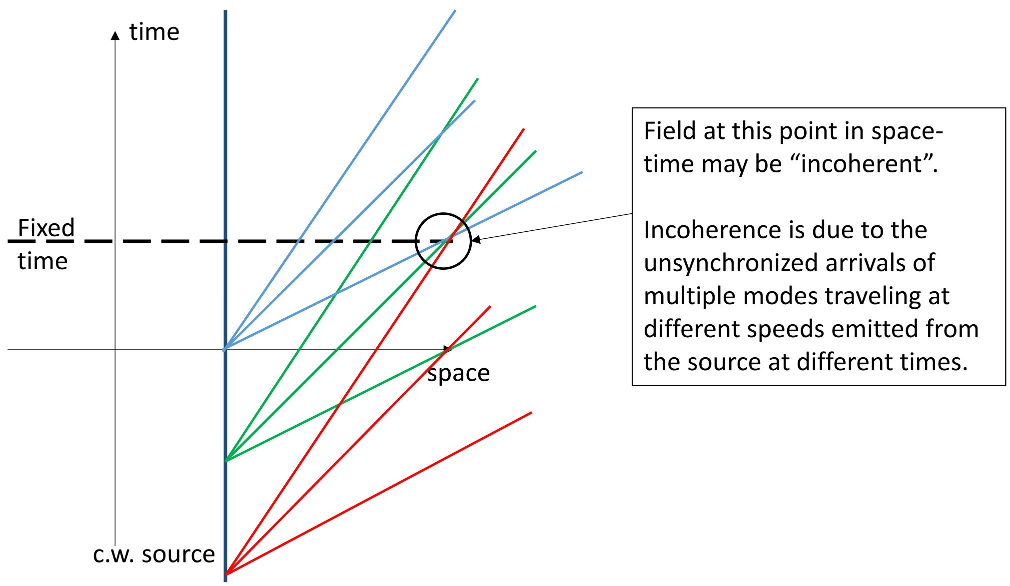

Figure 8 – Interpretation of the characteristics of the SME.

Since each chaos mode contributes some percentage of the true field, it may be reasonable to say that each ray path represents some portion of physical energy. However, inspection of the field equations shows that the wave speed eigenvalues do not appear. Instead, the material parameters couple the different modes together, causing information from one mode to mix and disperse into other modes. In the next section it is demonstrated that a linear combination of the original chaos modes will diagonalized the highest order terms in the SEM providing an interpretation that the rays represent propagation of a linear superposition of the original chaos modes.

Before moving on, an important observation is made regarding the characteristics. In applying the method of characteristics to any PDE system, one usually encounters one of three basic types of characteristic; elliptic, parabolic, and hyperbolic; corresponding to Laplace's equation, the heat or diffusion equation, and the wave equation respectively. Equations that describe propagating waves are typically hyperbolic, but they need not be. In fact, not all PDEs can be classified in one of these three categories and some defy classification. The equations describing acoustics and electromagnetics fall under the hyperbolic category. Key to this identification is a positive definite value for c^2. The derivation used the eigenvalue decomposition, which produced an infinite product of quadratic forms. Each positive eigenvalue produces a true hyperbolic characteristic and the usual interpretation of a light cone (more generally a Monge cone). If a negative eigenvalue is obtained, the corresponding characteristic would be elliptic in 4D, and for an imaginary or complex eigenvalue the characteristic does not belong to any category. In theory, this can happen, so each stochastic system needs to be carefully analyzed to ensure a full understanding and classification is achieved prior to applying the rays to a particular problem. One can make the educated guess that if the deviations from the main diagonal are small that a real eigenvalue spectrum would result, but again, each case should be independently vetted. One might be tempted to treat the complex or imaginary characteristic eigenvalues as contributing to attenuation. However, this interpretation requires rewriting Maxwell's equations in complex form, a common trick used to make differential equations easier to solve, with the true field being the real part of the solution. Since the derivation started with real valued fields, it would not be correct to interpret a complex eigen-speed as attenuation. In general, attenuation affects the amplitude along a path but not the geometry of the path, so one should not expect rays to be altered when attenuation is included.

5.2 Rotation of the chaos basis

A linear superposition of the original chaos coefficients, $\vec{B}^{(i)}$ and $\vec{D}^{(i)}$, that decouple the SME is desired. To make the steps clear each mode equation is presented in a list. The derivation proceeds assuming constant coefficients (generalization to be discussed later).

$$
\begin{array}{ll}
\dfrac{\partial \vec{B}^{(0)}}{\partial t} + \sum_{j=0}^{N} \vec{\nabla} \times \left(\mathrm{M}^{0j} \vec{D}^{(j)} \right) = 0 & \dfrac{\partial \vec{D}^{(0)}}{\partial t} - \sum_{j=0}^{N} \vec{\nabla} \times \left(\mathrm{R}^{0j} \vec{B}^{(j)} \right) = 0 \\
\vdots \qquad \vdots & \vdots \qquad \vdots \\
\dfrac{\partial \vec{B}^{(N)}}{\partial t} + \sum_{j=0}^{N} \vec{\nabla} \times \left(\mathrm{M}^{Nj} \vec{D}^{(j)} \right) = 0 & \dfrac{\partial \vec{D}^{(N)}}{\partial t} - \sum_{j=0}^{N} \vec{\nabla} \times \left(\mathrm{R}^{Nj} \vec{B}^{(j)} \right) = 0
\end{array}
$$

Let $N \to \infty$ to produce an independent linear superposition of each $\vec{B}^{(i)}$ and $\vec{D}^{(i)}$, defining a new set of fields. The coefficients of the magnetic (electric) field sum are denoted a_i^{α} (b_i^{α}), $\alpha = 0, \cdots, N, \cdots, \infty$ just as for i. It is clear that the same number of fields is required to describe the chaos problem. Latin (Greek) indices will refer to the original (new) fields. There is one N-dimensional vector for each new field, and the combination of all these vectors forms a generalized "rotation" in Hilbert space.

$$
\frac{\partial \left(a_0^0 \vec{B}^{(0)} + \cdots + a_N^0 \vec{B}^{(N)} \right)}{\partial t} + \sum_{j=0}^{N} \vec{\nabla} \times \left(\left(a_0^0 \mathrm{M}^{0j} + \cdots + a_N^0 \mathrm{M}^{Nj} \right) \vec{D}^{(j)} \right) = 0
$$

$$
\vdots
$$

$$
\frac{\partial \left(a_0^N \vec{B}^{(0)} + \cdots + a_N^N \vec{B}^{(N)} \right)}{\partial t} + \sum_{j=0}^{N} \vec{\nabla} \times \left(\left(a_0^N \mathrm{M}^{0j} + \cdots + a_N^N \mathrm{M}^{Nj} \right) \vec{D}^{(j)} \right) = 0
$$

$$\frac{\partial\left(b_0^0\vec{D}^{(0)}+\cdots+b_N^0\vec{D}^{(N)}\right)}{\partial t}-\sum_{j=0}^{N}\vec{\nabla}\times\left(\left(b_0^0\mathrm{R}^{0j}+\cdots+b_N^0\mathrm{R}^{Nj}\right)\vec{B}^{(j)}\right)=0$$
$$\vdots$$
$$\frac{\partial\left(b_0^N\vec{D}^{(0)}+\cdots+b_N^N\vec{D}^{(N)}\right)}{\partial t}-\sum_{j=0}^{N}\vec{\nabla}\times\left(\left(b_0^N\mathrm{R}^{0j}+\cdots+b_N^N\mathrm{R}^{Nj}\right)\vec{B}^{(j)}\right)=0$$

Next, set $a_0^\alpha\vec{B}^{(0)}+\cdots+a_N^\alpha\vec{B}^{(N)}=\vec{B}^{(\alpha)}$ and $b_0^\alpha\vec{D}^{(0)}+\cdots+b_N^\alpha\vec{D}^{(N)}=\vec{D}^{(\alpha)}$.

$$\frac{\partial\vec{B}^{(\alpha)}}{\partial t}+\sum_{j=0}^{N}\vec{\nabla}\times\left(\left(a_0^\alpha\mathrm{M}^{0j}+\cdots+a_N^\alpha\mathrm{M}^{Nj}\right)\vec{D}^{(j)}\right)=0$$

$$\frac{\partial\vec{D}^{(\alpha)}}{\partial t}-\sum_{j=0}^{N}\vec{\nabla}\times\left(\left(b_0^\alpha\mathrm{R}^{0j}+\cdots+b_N^\alpha\mathrm{R}^{Nj}\right)\vec{B}^{(j)}\right)=0$$

These equations can be decoupled if the following constraints on the coefficients is imposed.

$$a_0^\alpha\mathrm{M}^{0j}+\cdots+a_N^\alpha\mathrm{M}^{Nj}=\mathrm{M}^{(\alpha)}b_j^\alpha$$

$$b_0^\alpha\mathrm{R}^{0j}+\cdots+b_N^\alpha\mathrm{R}^{Nj}=\mathrm{R}^{(\alpha)}a_j^\alpha$$

In matrix form, these equations are,

$$\mathbf{M}^{\boldsymbol{T}}\cdot\boldsymbol{a}^{(\boldsymbol{\alpha})}=\mathrm{M}^{(\alpha)}\boldsymbol{b}^{(\boldsymbol{\alpha})}$$

$$\mathbf{R}^{\boldsymbol{T}}\cdot\boldsymbol{b}^{(\boldsymbol{\alpha})}=\mathrm{R}^{(\alpha)}\boldsymbol{a}^{(\boldsymbol{\alpha})}$$

These equations are combined to give,

$$(\mathbf{M}\cdot\mathbf{R})\cdot\boldsymbol{b}^{(\boldsymbol{\alpha})}=\mathrm{M}^{(\alpha)}\mathrm{R}^{(\alpha)}\boldsymbol{b}^{(\boldsymbol{\alpha})}$$
$$(\mathbf{R}\cdot\mathbf{M})\cdot\boldsymbol{a}^{(\boldsymbol{\alpha})}=\mathrm{M}^{(\alpha)}\mathrm{R}^{(\alpha)}\boldsymbol{a}^{(\boldsymbol{\alpha})}$$

$$\left(\boldsymbol{c}^{\mathbf{2}}\right)\cdot\boldsymbol{b}^{(\boldsymbol{\alpha})}=(C^2)^{(\alpha)}\boldsymbol{b}^{(\boldsymbol{\alpha})}$$
$$\left(\boldsymbol{c}^{\mathbf{2}}\right)^T\cdot\boldsymbol{a}^{(\boldsymbol{\alpha})}=(C^2)^{(\alpha)}\boldsymbol{a}^{(\boldsymbol{\alpha})}$$

I have used the fact that the stochastic material matrices are symmetric to drop the transpose, but note that, in general, they will not commute. These equations state that the weights for the new variables are eigenvectors of the wave speed matrix and its transpose with the same eigenvalue. The SME are expressed in with the new variables,

$$\frac{\partial\vec{B}^{(\alpha)}}{\partial t}+\mathrm{M}^{(\alpha)}\vec{\nabla}\times\vec{D}^{(\boldsymbol{\alpha})}=0$$

$$\frac{\partial \vec{D}^{(\alpha)}}{\partial t} - \mathrm{R}^{(\alpha)} \vec{\nabla} \times \vec{B}^{(\boldsymbol{\alpha})} = 0$$

Note that the inhomogeneous equation can be decoupled as well by using the coefficients $\boldsymbol{b}^{(\boldsymbol{\alpha})}$ to expand the current density modes, $\vec{J}^{(i)}$. Thus, a stochastic version of the inhomogeneous Maxwell's equations with constant background coefficients is equivalent to an infinite number of independent Maxwell fields. This means that any and all exact solutions can be applied to solving this class of stochastic equations, *e.g.* free space Green's function, plane wave solutions, interaction at a boundary between materials can all be carried over to the stochastic realm on a per mode basis. When it comes to numerical procedures, one does not need to develop new stochastic solvers. Rather, one can use existing solvers in parallel, solving for each mode independently.

For coordinate dependent parameters, the problem is a bit more involved. Taking linear superposition of each field by weighted addition of the equations requires bringing coefficients under the derivative operators. When the material parameters depend on coordinates one can expect the coefficients to have similar dependence.

$$a_0^\alpha \frac{\partial \vec{B}^{(0)}}{\partial t} + \cdots + a_N^\alpha \frac{\partial \vec{B}^{(N)}}{\partial t} = \frac{\partial\left(a_0^\alpha \vec{B}^{(0)} + \cdots + a_N^\alpha \vec{B}^{(N)}\right)}{\partial t} - \left\{\frac{\partial a_0^\alpha}{\partial t}\vec{B}^{(0)} + \cdots + \frac{\partial a_N^\alpha}{\partial t}\vec{B}^{(N)}\right\}$$

$$\begin{aligned} b_0^\alpha \vec{\nabla} \times \left(\mathrm{R}^{0j}\vec{B}^{(j)}\right) + \cdots + b_N^\alpha \vec{\nabla} \times \left(\mathrm{R}^{Nj}\vec{B}^{(j)}\right) \\ = \vec{\nabla} \times \left(\left(b_0^\alpha \mathrm{R}^{0j} + \cdots + b_N^\alpha \mathrm{R}^{Nj}\right)\vec{B}^{(j)}\right) - \left\{\vec{\nabla} b_0^\alpha \times \left(\mathrm{R}^{0j}\vec{B}^{(j)}\right) + \cdots + \vec{\nabla} b_N^\alpha \times \left(\mathrm{R}^{Nj}\vec{B}^{(j)}\right)\right\} \end{aligned}$$

Similarly for the other terms. Clearly, the introduction of inhomogeneous background parameters makes the rotation more complex and one should not expect constant coefficients to work. However, the highest order derivative terms will work out to be the same as in the previous case with constant parameters resulting in exactly the same characteristic structure.

It is clear from this section that the linear superposition derived represents the "mode" that propagates with the specific wave speed eigenvalue. In the case of a medium with purely constant, but uncertain parameters, this is all there is to the problem. Even in an inhomogeneous medium, rays with eigen-speeds correlate to propagation of information via these linear combination modes.

Even though the full set of Maxwell's equations do not diagonalize, field values predicted using first order ray theory only depend on geometric spread or ray bundles, so in this approximation the system can be considered approximately diagonal. Additionally, since the PE approximation ignores material gradients, and the expansion coefficients will depend on the material parameters, one might expect PE results to be approximately diagonal allowing one to run independent PE solvers for each mode $\vec{D}^{(\alpha)}$. This would allow UQ for complex problems to be treated very simply, but requires further validation.

5.3 Exact plane wave solution to SME

A review of the plane wave solution to Maxwell's equations in a source free region is presented as a starting point.

$$\vec{E} = \vec{E}_0 \exp i\left(\vec{k} \cdot \vec{x} - \omega t\right) \tag{5.1}$$

$$\vec{B} = \vec{B}_0 \exp i\left(\vec{k} \cdot \vec{x} - \omega t\right) \tag{5.2}$$

The divergence equations immediately produce the following condition obeyed by the polarization vectors and the wave vector.

$$\vec{k} \cdot \vec{E}_0 = 0 \tag{5.3}$$

$$\vec{k} \cdot \vec{B}_0 = 0 \tag{5.4}$$

Applying this solution to the time dependent equations leads to the following set of algebraic vector equations.

$$\vec{k} \times \vec{E}_0 = i\omega \vec{B}_0 \tag{5.5}$$

$$\vec{k} \times \vec{B}_0 = -i\omega\varepsilon\mu \vec{E}_0 \tag{5.6}$$

From the nature of the cross product, taking the dot product of Eq. (5.5) with $\vec{E}_0$, or Eq. (5.6) with $\vec{B}_0$, the following familiar relationship is derived.

$$\vec{E}_0 \cdot \vec{B}_0 = 0 \tag{5.7}$$

These solutions are described by three vectors, the constant field amplitudes and their mutual direction of travel. Taking the cross product of either Eq. (5.5) or (5.6) with $\vec{k}$, using the other to replace the right hand side, and applying a well-known vector identity gives the dispersion relation connecting the magnitude of $\vec{k}$ with the angular frequency, ω.

$$\vec{k} \cdot \vec{k} = \frac{\omega^2}{c^2} \tag{5.8}$$

These are all familiar results from any electrodynamics text [10].

Next, a similar solution is applied to the SME. A solution in the following form is assumed for the chaos modes.

$$\vec{D}^{(k)} = \vec{D}_0^{(k)} \exp i\left(\vec{k} \cdot \vec{x} - \omega t\right) \tag{5.9}$$

$$\vec{B}^{(k)} = \vec{B}_0^{(k)} \exp i\left(\vec{k} \cdot \vec{x} - \omega t\right) \tag{5.10}$$

Inserting these solutions into Eqs. (3.16) through (3.19) produces the following set of algebraic equations.

$$\omega D_{0x}^{(i)} - \sum \varphi^{(ilj)} R^{(l)} \left(k_y B_{0z}^{(j)} - k_z B_{0y}^{(j)}\right) = 0$$
$$\omega D_{0y}^{(i)} - \sum \varphi^{(ilj)} R^{(l)} \left(k_z B_{0x}^{(j)} - k_x B_{0z}^{(j)}\right) = 0$$
$$\omega D_{0z}^{(i)} - \sum \varphi^{(ilj)} R^{(l)} \left(k_x B_{0y}^{(j)} - k_y B_{0x}^{(j)}\right) = 0$$
$$\vdots$$
$$\omega B_{0x}^{(i)} + \sum \varphi^{(ilj)} M^{(l)} \left(k_y D_{0z}^{(j)} - k_z D_{0y}^{(j)}\right) = 0$$
$$\omega B_{0y}^{(i)} + \sum \varphi^{(ilj)} M^{(l)} \left(k_z D_{0x}^{(j)} - k_x D_{0z}^{(j)}\right) = 0$$
$$\omega B_{0z}^{(i)} + \sum \varphi^{(ilj)} M^{(l)} \left(k_x D_{0y}^{(j)} - k_y D_{0x}^{(j)}\right) = 0$$
$$\vdots$$

This set of equations can be put in matrix form.

$$\begin{bmatrix} \omega \mathbf{1_{3N}} & R \otimes \boldsymbol{K} \\ -M \otimes \boldsymbol{K} & \omega \mathbf{1_{3N}} \end{bmatrix} \begin{bmatrix} \boldsymbol{D} \\ \boldsymbol{B} \end{bmatrix} = 0 \tag{5.11}$$

A shorthand notation is used for the column vector,

$$\begin{bmatrix} \boldsymbol{D} \\ \boldsymbol{B} \end{bmatrix} \equiv \begin{bmatrix} \vdots \\ \vec{D}_0^{(i)} \\ \vec{D}_0^{(i+1)} \\ \vdots \\ \vec{B}_0^{(i)} \\ \vec{B}_0^{(i+1)} \\ \vdots \end{bmatrix}$$

The form of the matrix in Eq. (5.11) is identical to that of the characteristic matrix derived in chapter 4. To ensure a non-trivial solution for the polarization vectors the determinant of the matrix must vanish.

$$\det \begin{bmatrix} \omega \mathbf{1_{3N}} & R \otimes \boldsymbol{K} \\ -M \otimes \boldsymbol{K} & \omega \mathbf{1_{3N}} \end{bmatrix} = 0$$

Applying all the same steps and identities, the result of the determinant gives a constraint that must be obeyed to ensure freedom to select the field strength and direction.

$$\prod_{n=0}^{N} \left(\omega^2 - C_n^2 \left|\vec{k}\right|^2\right) = 0 \tag{5.12}$$

The allowed dispersion relations are governed by exactly the same eigenvalues as the characteristics or ray paths. Keeping in mind that a specific C_n^2 does not correspond to the original chaos mode but rather to the superposition that diagonalizes the SME. In hind sight, if one were to diagonalize the SME first, each mode could be solved independently with a plane wave solution and a single dispersion relationship though, it's nice to see the same logic pan out using different approaches. From the perspective of building the stochastic solution, one might wonder which mode to attribute each dispersion to and the answer is clearly all of them. In the rotated basis, the mode and dispersion are matched one-to-one.

A similar analysis can be applied to boundary conditions. The divergence equations imply that $\hat{n}\cdot\Delta\vec{D}^{(i)}=0$ and $\hat{n}\cdot\Delta\vec{B}^{(i)}=0$ for each chaos mode, where $\hat{n}$ is the normal to the boundary between two media.

Since the eigenvalue expansion decouples the modes, boundary conditions can be applied pairing modes in the spectrum of each random material. Thus, a full description can be generated from known exact solutions of multilayer problems.

6. DISCUSSION

6.1 Non-equivalence of the stochastic Eikonal and the Eikonal of the SME

The main results are encapsulated in chapters 3 through 5. Now I consider what would have been obtained if the chaos approach was applied directly to the ray equation or the Eikonal equation, assuming those as starting points. In the technical introduction the concept of applying stochasticity directly to ray paths was discussed. Valuable information regarding the behavior of propagating waves is contained in the ray equation for a smooth deterministic environment. The ray paths are connected to the full field equations through the Eikonal, or characteristic, of the original equations. Taken individually as equations it is always justified to elevate each to a stochastic DE. The question that arises is whether the three are still connected in any meaningful way. If not, does a stochastic ray equation still provide meaningful information about the field equations? I start this discussion by looking at stochastic versions of the Eikonal and ray equations using the polynomial chaos approach.

Applying the methods outlined in this report to the Eikonal, leads to a set of Eikonals, one for each chaos mode. The first question is what are the input parameters and are they related to the original input to SME. Already one is confronted with an ambiguity, does one take the local wave speed to be the stochastic parameter or the wave speed squared? For the purposes of this discussion, consider c^2 to be the input parameter. For many problems of interest the material has dielectric properties but no exotic magnetic properties, $\mu=\mu_0$, so treating c^2 as the input parameter is consistent with treating M as the input to Maxwell's equations. Expanding c^2 and the Eikonal in chaos modes, and projecting out onto a specific mode leads to the following hierarchy of equations.

$$\sum_{n,m=0}^{N}\varphi^{(pnm)}\,\partial_t\varphi^{(n)}\partial_t\varphi^{(m)}-\sum_{n,m=0}^{N}\sum_{l=0}^{N_c}\gamma^{(pnml)}c^{2\,(l)}\vec{\nabla}\varphi^{(n)}\cdot\vec{\nabla}\varphi^{(m)}=0 \tag{6.1}$$

Some obvious notation is introduced following that of chapter 3, and the quadruple product is defined, $\gamma^{(pnml)}\equiv\left\langle\Phi^{(p)}\middle|\Phi^{(n)}\Phi^{(n)}\Phi^{(l)}\right\rangle$. This system leads to $N(N+1)/2$ equations that couple all modes.

Next, consider the ray equation presented in chapter 4. Given the unique nature of the equations, the input parameter is c^2. The geodesic equation is used to represent any possible form of the ray equation consistent with equation (6.1). The Christoffel symbols are quadratic in the chaos basis due to the appearance of derivatives of c^2 multiplied by the inverse metric.

$$\frac{d^2(\xi^\mu)^{(n)}}{d\lambda^2} + \rho^{(npqml)}\left({\Gamma^\mu}_{\alpha\beta}\right)^{(p,q)} \frac{d(\xi^\alpha)^{(m)}}{d\lambda}\frac{d\left(\xi^\beta\right)^{(l)}}{d\lambda} = 0 \tag{6.2}$$

In equation (6.2), the quintuple product is introduced, $\rho^{(npqml)} = \left\langle \Phi^{(n)} \middle| \Phi^{(p)}\Phi^{(q)}\Phi^{(m)}\Phi^{(l)} \right\rangle$, and two sets of coordinates are present in (6.2). The coordinates x^μ provide local coordinate labels for points in a patch of space-time, whereas the variable ξ^μ is a solution to the geodesic equation and labels points on a specific curve in space-time. When evaluating the Christoffel symbols, one takes derivatives of the metric components everywhere using the operator $\partial/\partial x^\alpha$. These quantities are then expressed in terms of ξ^μ when included in the geodesic equation. This point is made to avoid confusion between the coordinate patch in which all quantities, including stochastic quantities, exist, and the coordinate labels of a specific curve that may be subjected to stochasticity. One may think that including stochastic terms in the metric makes tracking coordinates difficult. This distinction allows one to track the statistical change in a specific instance of a path in space-time given that the local wave speed contains uncertain parameters. Given a specific $c(x^\mu)$, one gets a specific $\xi^\mu(\lambda)$. One can think of space-time as being densely filled with possible trajectories. Uncertainty in $c(x^\mu)$ drives uncertainty in $\xi^\mu(\lambda)$ but does not invalidate the act of applying $\partial/\partial x^\alpha$ to $c(x^\mu)$.

There are now three distinct mathematical problems, each elevated to a stochastic system using the same methodology. Taken in isolation there is no inconsistency. One can study UQ of electromagnetic fields using (3.16) through (3.18), or study UQ of geodesics on a smooth manifold with uncertain geometric structure using (6.2). The field equations, Eikonal, and geodesic equations can each be studied in isolation. However, when these approaches are connected, one could run into trouble. The default thinking is that the rays describe the evolution of the Eikonal, which describes the evolution of the field equations. From the method of characteristics, these three things turn out to be connected in a logical manner. That connection is broken if one assumes that the UQ analysis can be started at any point, and results propagated into another domain. To better understand this, consider the Eikonal in more detail. Comparing the results of chapter 3 and equations (6.1) demonstrates that the applications of polynomial chaos and the method of characteristics do not commute. This is expressed in Figure 9.

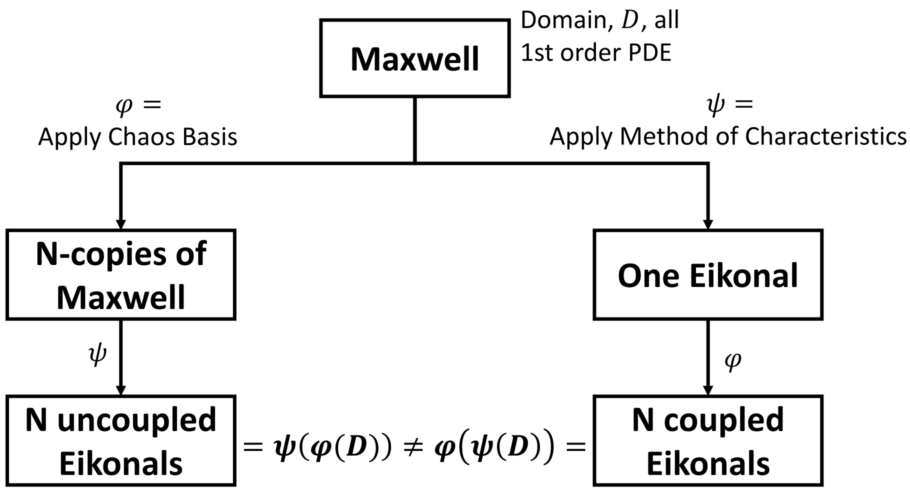

Figure 9 – Diagram mapping the actions of applying chaos and the method of characteristics to Maxwell's equations.

More generally, consider the process of applying chaos to all three systems. Figure 10 shows Maxwell's equations, the Eikonal equation, and geodesic equations, each with the application of stochastic effects by polynomial chaos. The abbreviations in Figure 10 are MC = Method of Characteristics, VC = Variational Calculus, and PC = Polynomial Chaos. The top row represents the 'classical' view of all three and their well understood connection. Viewing down the columns polynomial chaos is applied to each leading to stochastic versions of each. The far left column represents the results of chapters 3 and 4. The middle column shows the result of determining the rays of the stochastic Eikonal equation. Lastly, the far right column represents the study of stochastic geodesics.

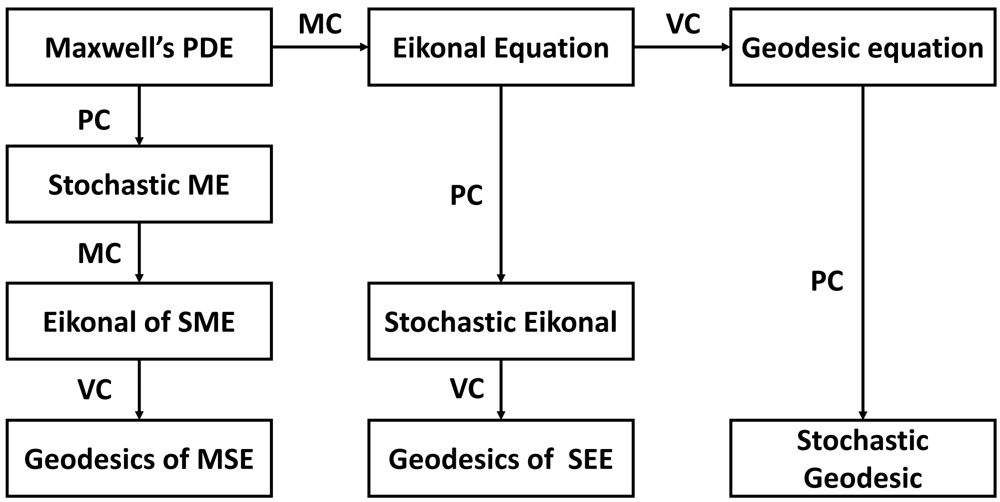

Figure 10 – Relationship between PDE, Eikonal, and Geodesics before stochastic methods and the effects of applying various methods after stochastic effects are included

Following these three distinct paths produces three different differential geometric systems, the geodesics of the SME = Stochastic Maxwell Equation, geodesics of the SEE = Stochastic Eikonal Equation, and finally, stochastic fluctuations of the 'classical' geodesics of Maxwell's equations.

ACKNOWLEDGEMENTS

The work is funded by the Office of Naval Research base program. The author would like to thank members of code 5314, Dr. Kragalott, Dr. Rao, and Charles Nelatury for helpful comments and reviews as this work was performed. The author would also like to thank summer interns Maxwell Block and Ritvik Gunturu for their participation.

REFERENCES

1. V. Perlick, *Ray Optics, Fermat's Principle, and Applications to General Relativity* (Springer-Verlag, Berlin, 2000)

2. M. Born and E. Wolf, *Principles of Optics: Electromagnetic Theory of Propagation Interference and Diffraction of Light 6th Edition*, (Pergamon Press, Oxford, 1980)

3. I. Tolstoy and C.S. Clay, *Ocean Acoustics, Theory and Experiment in Underwater Sound* (McGraw-Hill, New York, 1966).

4. D.R. Bergman, *Application of Differential Geometry to Acoustics: Development of a Generalized Paraxial Ray-Trace Procedure from Geodesic Deviation*, NRL/MR/7140—05-8835, Approved for public release – Distribution Unlimited, 2005

5. R.W. White, "Acoustic ray tracing in moving inhomogeneous fluids", Journal of the Acoustical Society of America, 53, 1700-1704, (1972).

6. V.M. Babich and A.P. Kiselev, Elastic Waves High Frequency Theory (CRC Press, Boca Raton, 2018)

7. R. Courant & D. Hilbert, *Methods of Mathematical Physics Volumes I and II* (John Wiley and Sons, New York, 1984)

8. A. McDaniel and A. Mahalov. "Stochastic mirage phenomenon in a random medium". Optics Letters, Vol. 42, No. 10, 2002-2005 (2017).

9. N. Wiener, "The Homogeneous Chaos", American Journal of Mathematics, Vol. 60, No. 4, 897-936 (1938).

10. J.D. Jackson, *Classical Electrodynamics Second Edition* (Wiley, New York, 1975).

11. F.J. Ryan, *Analysis of Electromagnetic Propagation Over Variable Terrain Using The Parabolic Wave Equations*, Technical Report 1453¸ Approved for public Release – Distribution Unlimited, (1991).

12. J. Baez and J.P. Muniain, *Gauge Fields, Knots and Gravity* (World Scientific, Singapore, 1994).

13. G.A. Deschamps, "Electromagnetism and differential forms", Proceedings of the IEEE, Vol. 69, No. 6, 676-696 (1981).

14. K.F. Warnick and P. Russer, "Differential Forms and Electromagnetic Field Theory", Progress In Electromagnetics Research, Vol. 148, 83-112 (2014).

15. M. Haider and J.A. Russer, "Differential form representation of stochastic electromagnetic fields", Advances in Radio Science, 15, 21-28 (2017).

16. H. Flanders, *Differential Forms with Applications to the Physical Sciences* (Academic Press, Cambridge, 1963).

17. O.C. Pin, "Curvature and Mechanics", Advances in Mathematics, 15, 269-311 (1975).

18. K.F. Warnick, R.H. Selfridge, and D.V. Arnold, "Teaching electromagnetic field theory using differential forms", IEEE Transactions on Education, Vol. 40, No. 1, 53-68 (1997).

19. D. Baldomir, "Differential forms and electromagnetism in 3-dimensional Euclidean space R^3", Science IEE Proceedings, Vol. 133, Pt. A, No. 3, 139-143 (1986).

20. D.B. Nguyen, "Relativistic constitutive relations, differential forms, and the p-compound", American Journal of Physics, 60 (12), 1137-1144 (1992).

21. W.L. Burke, “Manifestly parity invariant electromagnetic theory and twisted tensors”, Journal of Mathematical Physics, 24 (1), 65-69 (1983).

22. K.F. Warnick, R.H. Selfridge, and D.V. Arnold, “Electromagnetic boundary conditions and differential forms”, IEE Proceedings Microwaves, Antennas, and Propagation, Vol. 142, No. 4, 326-332 (1995).

23. I.V. Lindell and B. Jancewicz, “Electromagnetic boundary conditions in differential form formalism”, European Journal of Physics, 21, 83-89 (2000)

24. A. Papoulis, *Probability, Random Variables, and Stochastic Processes 2nd Edition* (McGraw-Hill Book Company, New York, 1984)

25. G. Gradoni, J. Russer, M.H. Baharuddin, M. Haider, P. Russer, C. Smartt, S.C. Creagh, G. Tanner and D.W.P. Thomas, “Stochastic electromagnetic field propagation – measurement and modelling”, Philosophical Transactions of the Royal Society A, 376:20170455

26. A.I. Sokolovsky and A.A Stupka, “Classical fluctuation electrodynamics”, Condensed Matter Physics, Vol. 8, No. 4 (44), 685-700 (2005).

27. J.A. Russer and P. Russer, “Modeling of Noisy EM Field Propagation Using Correlation Information”, IEEE Transactions on Microwave Theory and Techniques, Vol. 63, No. 1, 76-89 (2015)

28. M Yao, I. Toselli, and O. Korotkova, “Propagation of electromagnetic stochastic beams in anisotropic turbulence”, Optics Express 31608, Vol. 22, No. 6, DOI:10.1364/OE.22.031608 (2014).

29. A. McDaniel and A. Mahalov, “Lensing effects in a random inhomogeneous medium”, Optics Express 28157. Vol. 25, No. 23, doi.org/10.1364/OE.25.028157 (2017).

30. X. Yi and I.B. Djordjevic, “Power spectrum of refractive-index fluctuations in turbulent ocean and its effect on optical scintillation”, Optics express 10188, Vol. 26, No. 8, doi.org/10.1364/OE.26.010188 (2018).

31. S. Sahin and O. Korotkova, “Fluctuations in the instantaneous Stokes parameters of stochastic electromagnetic beams propagation in the turbulent atmosphere”, Proceedings of SPIE 7200, Atmospheric Propagation of Electromagnetic Waves III, doi: 10.1117/12.811168 (2009).

32. M. Enstedt and N. Wellander, “Uncertainty Quantification of Radio Propagation Using Polynomial Chaos”. Progress In Electromagnetics Research M, Vol. 50, 205-213 (2016).

33. A. Kaintura, T. Dhaene, and D. Spina,”Review pf Polynomial Chaos-Based Methods for Uncertainty Quantification in Modern Integrated Circuits, Electronics, 7, 30, doi:10.3390/electronics7030030 (2018).

34. T. Jain, R.G. Patel and J. Trivedi, “Application of polynomial chaos theory as an accurate and computationally efficient proxy model for heterogeneous steam-assisted gravity drainage reservoirs”, Energy Science and Engineering, 5(5), 270-289 (2017).

35. M.M.R. Williams, "Polynomial chaos functions and stochastic differential equations", Annals of Nuclear Engineering, 33, 774-785 (2006).

36. D. Xiu and G.E. Karniadakis, "Modeling uncertainty in flow simulations via generalized polynomial chaos", Journal of Computational Physics, 187, 137-167 (2003).

37. X. Wan and G.E. Karniadakis, "An adaptive multi-element generalized polynomial chaos method for stochastic differential equations", Journal of Computational Physics, 209, 617-642 (2005).

38. D. Xiu and G.E. Karniadakis, "The Wiener-Askey Polynomial Chaos for Stochastic Differential Equations", SIAM Journal of Scientific Computing, Vol. 24. No. 2, 619-644 (2002).

39. R. Ghanem, "Ingredients for a general purpose stochastic finite element implementation", Computer Methods in Applied Mechanics and Engineering, 168, 19-34 (1999).

40. R. Ghanem and P.D. Spanos, *Stochastic Finite Elements A Spectral Approach Revised Edition* (Dover, New York, 2003).

41. L. Carlitz, "The product of several Hermite or Laguerre polynomials", Monatshefte für Mathematik, 66, 393-396 (1962).

42. R.D. Lord, "Integrals of products of Laguerre polynomials", Mathematics of Computation, 14, 375-376 (1960).

43. S. Dong and R. Lemus, "The Overlap Integral of Three Associated Legendre Polynomials", Applied Mathematics Letters, 15, 541-546 (2002).

44. P. Lee, S. Ong and H.M. Srivastava, "Some Integrals of the Products of Laguerre Polynomials", International Journal of Computer Mathematics, Vol. 78, 303-321 (2001).

45. S. Beuchler, T. Haubold and V. Pillwein, "Recursion Formulas for Integrated Products of Jacobi Polynomials", Constructive Approximation, doi.org/10.1007/s00365-023-09655-z (2023).

46. D.R. Bergman, "Internal symmetry in acoustical ray theory", Wave Motion, 43, 508-516 (2005).

47. T.L. Foreman, "An exact ray theoretical formulation of the Helmholtz equation", Journal of the Acoustical Society of America, 86, 234-246 (1989).

48. W.L. Burke, *Applied Differential Geometry*, (Cambridge, Cambridge, 1985).

49. M. Spivak, *A Comprehensive Introduction to Differential Geometry Volumes 1 through 5* (Publish or Perish, , 1999)

51. C.W. Misner, K.S. Thorne, and J.A. Wheeler, *Gravitation* (Freeman, New York, 1970).

51. B. O'Neill, *Elementary Differential Geometry* (Academic Press, San Diego, 1966).

A. THE METHOD OF CHARACTERISTICS APPLIED TO MAXWELL'S EQUATIONS

The method of characteristics is a general procedure for developing solutions to systems of quasi-linear partial differential equations (PDE). A complete description can be found in Volume II of Courant and Hilbert "Methods of Mathematical Physics" [7]. The term quasi-linear means that the equations are linear in the highest derivative of the fields, lower order derivatives can be non-linear. Consider a PDE system of highest order m describing F fields propagating in N-dimensional space, see Figure 11. The description of solutions for a PDE system involve specifying the field and its derivative up to order m-1 on some N-1 dimensional hyper surface, Σ. This surface of initial data can be used as a coordinate surface leaving one dimension left, described locally by the gradient of the initial surface. Figure 11 illustrates the situation. Using this approach, one can form a description of the highest derivative in terms of the initial data. Expressing the original PDE in this new coordinate system one then imposes the constraint that the equation not be invertible. The criterion for the PDE to be non-trivial is expressed by stating that the determinant of the coefficients of the highest order normal derivatives vanish. This leads to the characteristic condition for the PDE. When applied to hyperbolic PDE evolving in space-time, the resulting characteristic is identified as a wave front and its gradient field with ray paths, also called bicharacteristics. The most popular application is to first and second order system, that lead to various types of wave propagation including; the equations of hydrodynamics for a Newtonian fluid, Maxwell's equations, and the wave equation in various forms for liquids and solids.

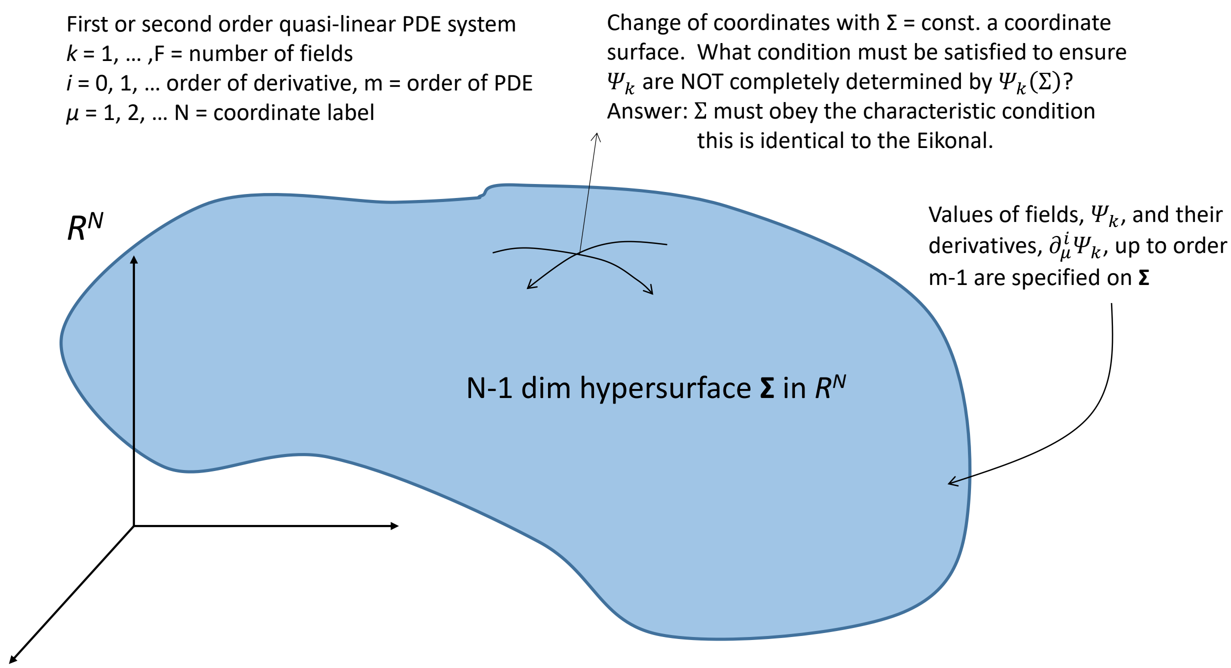

Figure 11 – Standard description of a characteristic surface for a PDE and the relation to Cauchy data

In this appendix, I present a detailed derivation of the characteristics for Maxwell's classical equation, as well as the SME presented in this report for the case $N = 2$. This presentation is meant to serve as a "recipe" for applying the technique that the reader may use in the analysis of other PDEs. This appendix also provides details not presented in the main text in support of derivations.

The method is illustrated on Maxwell's equations in free space in the absence of sources with the components of $\vec{E}$ and $\vec{H}$ treated as independent fields, and to Maxwell's equations expressed in terms of a gauge potential. To apply the method of characteristics, assign an index to each independent field (a total of 6 degrees of freedom for the original Maxwell equations). The fields are placed in a large vector and given an index, purely as a book keeping device, as follows.

$$[H_x \quad H_y \quad H_z \quad E_x \quad E_y \quad E_z]^T$$

By this convention, field 1 is H_x and field 4 is E_x, *etc*. The first step in developing the characteristic equation is to determine a set of matrixes that contain the coefficients of each derivative of the fields listed above. These will be *N*-by-*N* matrices (where *N* = number of fields, in this case 6). The row index labels the specific equation in the same order as the fields. For any given row, simply walk through the equation and place the coefficients of the derivative of each field in the appropriate column slot, corresponding to that field index. For the above convention, the component differential equations are listed below.

$$\mu\partial_t H_x + \partial_y E_z - \partial_z E_y = 0 \tag{A.1}$$

$$\mu\partial_t H_y + \partial_z E_x - \partial_x E_z = 0 \tag{A.2}$$

$$\mu\partial_t H_z + \partial_x E_y - \partial_y E_x = 0 \tag{A.3}$$

$$\varepsilon\partial_t E_x - \partial_y H_z + \partial_z H_y = 0 \tag{A.4}$$

$$\varepsilon\partial_t E_y - \partial_z H_x + \partial_x H_z = 0 \tag{A.5}$$

$$\varepsilon\partial_t E_z - \partial_x H_y + \partial_y H_x = 0 \tag{A.6}$$

The four derivative matrices are labeled $\boldsymbol{A^t}$, $\boldsymbol{A^x}$, *etc*. To fill each matrix, simply look for derivatives of each field with respect to that matrix index and write the coefficient in the appropriate row and column. Starting with the time derivative, Eq. (A.1) contains only the time derivative of field 1, H_x, *etc*. Hence, in this case, the time matrix is diagonal.

$$\boldsymbol{A^t} = \begin{bmatrix} \mu & 0 & 0 & 0 & 0 & 0 \\ 0 & \mu & 0 & 0 & 0 & 0 \\ 0 & 0 & \mu & 0 & 0 & 0 \\ 0 & 0 & 0 & \varepsilon & 0 & 0 \\ 0 & 0 & 0 & 0 & \varepsilon & 0 \\ 0 & 0 & 0 & 0 & 0 & \varepsilon \end{bmatrix} = \begin{bmatrix} \mu\mathbf{I_3} & \mathbf{0} \\ \mathbf{0} & \varepsilon\mathbf{I_3} \end{bmatrix}$$

A short hand notation is introduced where $\mathbf{I_3}$ is the 3D identity matrix and $\mathbf{0}$ represents a 3-by-3 matrix full of zeros. The shorthand $\boldsymbol{\mu} = \mu\mathbf{I_3}$ is used to avoid writing the identity. The other derivative matrices are now filled.

$$\boldsymbol{A^x} = \begin{bmatrix} & \mathbf{0} & & 0 & 0 & 0 \\ & & & 0 & 0 & -1 \\ & & & 0 & 1 & 0 \\ 0 & 0 & 0 & & & \\ 0 & 0 & 1 & & \mathbf{0} & \\ 0 & -1 & 0 & & & \end{bmatrix}$$

The reader can verify these coefficients. For example, the first equation does not contain any derivatives with respect to *x*, leading to a row of zeros. In the second equation, there is an *x* derivative of E_z, which is the 6th field. The coefficient of this term is -1, hence, the (2, 6) entry. Similar steps lead to the following for the other two derivative coefficient matrices.

$$\boldsymbol{A^y} = \begin{bmatrix} & \mathbf{0} & & 0 & 0 & 1 \\ & & & 0 & 0 & 0 \\ & & & -1 & 0 & 0 \\ 0 & 0 & -1 & & & \\ 0 & 0 & 0 & & \mathbf{0} & \\ 1 & 0 & 0 & & & \end{bmatrix}$$

$$\boldsymbol{A^z} = \begin{bmatrix} & \mathbf{0} & & 0 & -1 & 0 \\ & & & 1 & 0 & 0 \\ & & & 0 & 0 & 0 \\ 0 & -1 & 0 & & & \\ 1 & 0 & 0 & & \mathbf{0} & \\ 0 & 0 & 0 & & & \end{bmatrix}$$

The characteristic equation is derived by taking the determinant of $A^\alpha \partial_\alpha \varphi$ and setting it to zero. The Greek index $\alpha = 0, 1, 2, 3$ with 0 = *t* and 1, 2, 3 for space indices. The complete characteristic matrix for the system of Eqs. (A.1 – A.6) is given below in Eq. (A.7).

$$\begin{bmatrix} \mu\partial_t\varphi & 0 & 0 & 0 & -\partial_z\varphi & \partial_y\varphi \\ 0 & \mu\partial_t\varphi & 0 & \partial_z\varphi & 0 & -\partial_x\varphi \\ 0 & 0 & \mu\partial_t\varphi & -\partial_y\varphi & \partial_x\varphi & 0 \\ 0 & \partial_z\varphi & -\partial_y\varphi & \varepsilon\partial_t\varphi & 0 & 0 \\ -\partial_z\varphi & 0 & \partial_x\varphi & 0 & \varepsilon\partial_t\varphi & 0 \\ \partial_y\varphi & -\partial_x\varphi & 0 & 0 & 0 & \varepsilon\partial_t\varphi \end{bmatrix} \tag{A.7}$$

An interesting and potentially useful pattern emerges with the space derivative matrices. The lower left block is the negative of the upper right block. In fact this is true for each of the derivative coefficient matrices $\boldsymbol{A^j}$, *j* = 1, 2, 3. Defining lowercase matrices

$$\boldsymbol{a^x} = \begin{bmatrix} 0 & 0 & 0 \\ 0 & 0 & -1 \\ 0 & 1 & 0 \end{bmatrix} \quad \boldsymbol{a^y} = \begin{bmatrix} 0 & 0 & 1 \\ 0 & 0 & 0 \\ -1 & 0 & 0 \end{bmatrix} \quad \boldsymbol{a^z} = \begin{bmatrix} 0 & -1 & 0 \\ 1 & 0 & 0 \\ 0 & 0 & 0 \end{bmatrix}$$

the space derivate matrices are written in compact form,

$$\boldsymbol{A}^x = \begin{bmatrix} \boldsymbol{0} & \boldsymbol{a}^x \\ -\boldsymbol{a}^x & \boldsymbol{0} \end{bmatrix} \quad \boldsymbol{A}^y = \begin{bmatrix} \boldsymbol{0} & \boldsymbol{a}^y \\ -\boldsymbol{a}^y & \boldsymbol{0} \end{bmatrix} \quad \boldsymbol{A}^z = \begin{bmatrix} \boldsymbol{0} & \boldsymbol{a}^z \\ -\boldsymbol{a}^z & \boldsymbol{0} \end{bmatrix}$$

The characteristic matrix may be written in a compact form.

$$\begin{bmatrix} \boldsymbol{\mu}\partial_t\varphi & \vec{\boldsymbol{a}}\cdot\vec{\nabla}\varphi \\ -\vec{\boldsymbol{a}}\cdot\vec{\nabla}\varphi & \boldsymbol{\varepsilon}\partial_t\varphi \end{bmatrix} \tag{A.8}$$

Lastly, note that the little matrices, $\boldsymbol{a}^{\boldsymbol{i}}$ i = 1, 2, 3, are the generators of the Lie Algebra for the special orthogonal group in 3-D, *SO*(3), which form rotation matrices connected to the identity (*i.e.* parity preserving).

Applying this technique to the SME follows the same route, but with an infinite number of fields. A good choice of ordering will make things more manageable. Before moving on to the general case, I demonstrate the approach applied to SME with $N = 1$, *i.e.* only 2 chaos basis fields. In this case, each vector will have a partner leading to 12 degrees of freedom. These fields are denoted, $\vec{H}^0$, $\vec{H}^1$, $\vec{E}^0$, and $\vec{E}^1$ and are indexed as follows.

$$\begin{bmatrix} H_x^0 & H_y^0 & H_z^0 & H_x^1 & H_y^1 & H_z^1 & E_x^0 & E_y^0 & E_z^0 & E_x^1 & E_y^1 & E_z^1 \end{bmatrix}^T$$

In vector form, the set of hierarchical equations may be written,

$$\mu^{00}\partial_t\vec{H}^0 + \mu^{01}\partial_t\vec{H}^1 + \vec{\nabla}\times\vec{E}^0 + \partial_t\mu^{00}\vec{H}^0 + \partial_t\mu^{01}\vec{H}^1 = 0 \tag{A.9}$$

$$\mu^{10}\partial_t\vec{H}^0 + \mu^{11}\partial_t\vec{H}^1 + \vec{\nabla}\times\vec{E}^1 + \partial_t\mu^{10}\vec{H}^0 + \partial_t\mu^{11}\vec{H}^1 = 0 \tag{A.10}$$

$$\varepsilon^{00}\partial_t\vec{E}^0 + \varepsilon^{01}\partial_t\vec{E}^1 - \vec{\nabla}\times\vec{H}^0 + \partial_t\varepsilon^{00}\vec{E}^0 + \partial_t\varepsilon^{01}\vec{E}^1 = 0 \tag{A.11}$$

$$\varepsilon^{10}\partial_t\vec{E}^0 + \varepsilon^{11}\partial_t\vec{E}^1 - \vec{\nabla}\times\vec{H}^1 + \partial_t\varepsilon^{10}\vec{E}^0 + \partial_t\varepsilon^{11}\vec{E}^1 = 0 \tag{A.12}$$

Writing down individual component equations is not necessary as long as one keeps track of the curl in each equations. The method of characteristics tracks the highest order derivatives of the fields, the last two terms in equations A.9 through A.12 have no effect on the results. The resulting characteristic matrix are written in terms of the basic building blocks derived for the free space Maxwell equation.

$$\begin{bmatrix} \begin{pmatrix} \boldsymbol{\mu}^{00}\partial_t\varphi & \boldsymbol{\mu}^{01}\partial_t\varphi \\ \boldsymbol{\mu}^{10}\partial_t\varphi & \boldsymbol{\mu}^{11}\partial_t\varphi \end{pmatrix} & \begin{pmatrix} \vec{\boldsymbol{a}}\cdot\vec{\nabla}\varphi & \mathbf{0} \\ \mathbf{0} & \vec{\boldsymbol{a}}\cdot\vec{\nabla}\varphi \end{pmatrix} \\ \begin{pmatrix} -\vec{\boldsymbol{a}}\cdot\vec{\nabla}\varphi & \mathbf{0} \\ \mathbf{0} & -\vec{\boldsymbol{a}}\cdot\vec{\nabla}\varphi \end{pmatrix} & \begin{pmatrix} \boldsymbol{\varepsilon}^{00}\partial_t\varphi & \boldsymbol{\varepsilon}^{01}\partial_t\varphi \\ \boldsymbol{\varepsilon}^{10}\partial_t\varphi & \boldsymbol{\varepsilon}^{11}\partial_t\varphi \end{pmatrix} \end{bmatrix} \tag{A.13}$$

A simple pattern emerges which is verified by induction.

$$\begin{bmatrix} \begin{pmatrix} \boldsymbol{\mu}^{00}\partial_t\varphi & \cdots & \boldsymbol{\mu}^{0N}\partial_t\varphi \\ \vdots & \ddots & \vdots \\ \boldsymbol{\mu}^{N0}\partial_t\varphi & \cdots & \boldsymbol{\mu}^{NN}\partial_t\varphi \end{pmatrix} & \begin{pmatrix} \vec{\boldsymbol{a}}\cdot\vec{\nabla}\varphi & \mathbf{0} & \mathbf{0} \\ \mathbf{0} & \ddots & \mathbf{0} \\ \mathbf{0} & \mathbf{0} & \vec{\boldsymbol{a}}\cdot\vec{\nabla}\varphi \end{pmatrix} \\ \begin{pmatrix} -\vec{\boldsymbol{a}}\cdot\vec{\nabla}\varphi & \mathbf{0} & \mathbf{0} \\ \mathbf{0} & \ddots & \mathbf{0} \\ \mathbf{0} & \mathbf{0} & -\vec{\boldsymbol{a}}\cdot\vec{\nabla}\varphi \end{pmatrix} & \begin{pmatrix} \boldsymbol{\varepsilon}^{00}\partial_t\varphi & \cdots & \boldsymbol{\varepsilon}^{0N}\partial_t\varphi \\ \vdots & \ddots & \vdots \\ \boldsymbol{\varepsilon}^{N0}\partial_t\varphi & \cdots & \boldsymbol{\varepsilon}^{NN}\partial_t\varphi \end{pmatrix} \end{bmatrix} \tag{A.14}$$

To illustrate how the method is applied to a second order PDE, consider Maxwell's equations expressed in terms of the 4-vector potential. To determine the characteristics of Maxwell's equations in this representation, the inhomogeneous equations are used, expressing the fields in terms of the potentials.

$$\vec{B} = \vec{\nabla} \times \vec{A} \tag{A.15}$$

$$E = -\vec{\nabla}\psi - \frac{\partial \vec{A}}{\partial t} \tag{A.16}$$

Inserting these into the inhomogeneous equations and using the constitutive equations leads to the following set of second order equations for the potential functions.

$$\varepsilon\vec{\nabla}\cdot\left[\vec{\nabla}\psi + \frac{\partial \vec{A}}{\partial t}\right] + \rho_f = 0 \tag{A.17}$$

$$R\left[\vec{\nabla}\left(\vec{\nabla}\cdot\vec{A}\right) - \nabla^2\vec{A}\right] + \varepsilon\frac{\partial}{\partial t}\left[\vec{\nabla}\psi + \frac{\partial \vec{A}}{\partial t}\right] - \vec{J}_f = 0 \tag{A.18}$$

Each derivative of a field gets an associated factor of $\partial_\mu\varphi$. Second derivatives will get two such factors each stemming from a coordinate transformation where the surface φ is a coordinate surface. A shorthand notation is introduced, $\vec{\nabla}\varphi = \vec{p}$ and $\partial_t\varphi = p_0$.

$$\begin{bmatrix} \varepsilon p^2 & \varepsilon p_0 p_x & \varepsilon p_0 p_y & \varepsilon p_0 p_z \\ \varepsilon p_0 p_x & \varepsilon p_0^2 + R(p_x^2 - p^2) & R p_x p_y & R p_x p_z \\ \varepsilon p_0 p_y & R p_x p_y & \varepsilon p_0^2 + R\left(p_y^2 - p^2\right) & R p_y p_z \\ \varepsilon p_0 p_z & R p_x p_z & R p_y p_z & \varepsilon p_0^2 + R(p_z^2 - p^2) \end{bmatrix} \tag{A.19}$$

It turns out that the determinant of Eq. (A.19) is identically zero, implying no constraint on the surface. The reason for this is that a gauge has not yet been selected. The original set of Maxwell's equations are an overdetermined system. This is reflected by the fact that changing the potential by a specific field transformation leaves the entire set of equations unaltered. There are an infinite number of gauges to choose from, the three most common are,

$$\partial_t(\varepsilon\psi) + \vec{\nabla}\cdot\left(R\vec{A}\right) = 0 \qquad \text{Lorentz} \tag{A.20}$$

$$\vec{\nabla}\cdot\vec{A} = 0 \qquad \text{Coulomb} \tag{A.21}$$

$$\psi = 0 \qquad \text{Temporal} \tag{A.22}$$

Imposing the Coulomb gauge eliminates $\vec{\nabla}\cdot\vec{A}$ from all equations, which eliminates most off-diagonal terms, leading to the following characteristic.

$$\begin{bmatrix} \varepsilon p^2 & 0 & 0 & 0 \\ \varepsilon p_0 p_x & \varepsilon p_0^2 - p^2 R & 0 & 0 \\ \varepsilon p_0 p_y & 0 & \varepsilon p_0^2 - p^2 R & 0 \\ \varepsilon p_0 p_z & 0 & 0 & \varepsilon p_0^2 - p^2 R \end{bmatrix} \tag{A.23}$$

Applying the temporal gauge leads to elimination of the left column completely. This isn't very helpful since one now has an over determined system. However, recognizing that the first equation serves as a constraint

$$\begin{bmatrix} \varepsilon p_0^2 + R(p_x^2 - p^2) & R p_x p_y & R p_x p_z \\ R p_x p_y & \varepsilon p_0^2 + R\left(p_y^2 - p^2\right) & R p_y p_z \\ R p_x p_z & R p_y p_z & \varepsilon p_0^2 + R(p_z^2 - p^2) \end{bmatrix} \tag{A.24}$$

Lastly, applying the Lorentz gauge condition (for taken from Dechamps [13]) leads to the following set of equations for the potentials.

$$\begin{bmatrix} \varepsilon p_0^2 - R p^2 & 0 & 0 & 0 \\ 0 & \varepsilon p_0^2 - R p^2 & 0 & 0 \\ 0 & 0 & \varepsilon p_0^2 - R p^2 & 0 \\ 0 & 0 & 0 & \varepsilon p_0^2 - R p^2 \end{bmatrix} \tag{A.25}$$

For this gauge, the fields completely decouple at the highest order giving a diagonal characteristic matrix. All these forms give the same light cone structure by forcing the determinant to vanish.

$$(p_0^2 - c^2 p^2) = 0$$

It is somewhat reassuring that all gauges lead to the same light cone structure (more generally null hypersurface structure). It should also be noted that with an infinite number of possible gauges the form of the potential equation is not fixed and can be made more or less complex by selecting an appropriate gauge. All this does is restrict the degrees of freedom in A^μ.

B. USEFUL MATRIX IDENTITIES

The derivation of the characteristic equation(s) requires evaluating the determinant of the characteristic matrix. This appendix lists several useful relationships and identities that are make this task tractable, especially for infinite dimensional matrices.

The determinant of a block matrix can be reduced or simplified under certain conditions. Consider a square matrix represented in block form.

$$M = \begin{bmatrix} A & B \\ C & D \end{bmatrix} \tag{B.1}$$

For this report only the case where M has an even number of rows and columns and the blocks are half the size of the full matrix is needed. In the most general case, the determinant of M can be expressed in terms of the smaller blocks.

$$\det(M) = \begin{cases} \det(A)\det(D - CA^{-1}B) & \text{when } A \text{ is invertable} \\ \det(A - BD^{-1}C)\det(D) & \text{when } D \text{ is invertable} \end{cases} \tag{B.2}$$

If either $AB = BA$ or $CD = DC$ the determinant simplifies.

$$\det(M) = \det(AD - BC) \tag{B.3}$$

In general, a matrix can be written in terms of its eigenvalues and eigenvectors.

$$M = Q\Lambda Q^{-1} \tag{B.4}$$

In Eq. (B.4), the matrix Λ is a diagonal matrix containing the eigenvalues, λ_i, of M and Q, a matrix with the normalized eigenvectors, $\hat{\mathrm{v}}_i$, of M in each column.

The determinant of a product of matrices is equal to the product of the determinants of the individual matrices. A consequence of this is that one can permute the factors inside of the determinant.

$$\det(M_1 \cdots M_N) = \det(M_1) \cdots \det(M_N) = \det\left(M_1 \cdots M_j \cdots M_i \cdots M_N\right) \tag{B.5}$$

Using Eq. (B.5) it is easy to prove the well-known result expressed in equation (B.6).

$$\det(M) = \lambda_1^{n_1} \cdots \lambda_N^{n_N} \tag{B.6}$$

The powers, n_i, are the multiplicity of the eigenvalues.

One often encounter matrices that are built up from the direct product or direct sum of smaller matrices. The direct product of two square matrices, A and B, of sizes $N_1 \times N_1$ and $N_2 \times N_2$ is a square matrix of size $(N_1 N_2) \times (N_1 N_2)$. The direct product of A and B is defined as,

$$A \otimes B = \begin{bmatrix} a_{11}B & \cdots & a_{1N_1}B \\ \vdots & \ddots & \vdots \\ a_{N_1 1}B & \cdots & a_{N_1N_1}B \end{bmatrix}$$
$$= \begin{bmatrix} a_{11}b_{11} & \cdots & a_{11}b_{1N_2} & & a_{1N_1}b_{11} & \cdots & a_{1N_1}b_{1N_2} \\ \vdots & \ddots & \vdots & \cdots & \vdots & \ddots & \vdots \\ a_{11}b_{N_2 1} & \cdots & a_{11}b_{N_2N_2} & & a_{1N_1}b_{N_2 1} & \cdots & a_{1N_1}b_{N_2N_2} \\ & \vdots & & \ddots & & \vdots & \\ a_{N_1 1}b_{11} & \cdots & a_{N_1 1}b_{1N_2} & & a_{N_1N_1}b_{11} & \cdots & a_{N_1N_1}b_{1N_2} \\ \vdots & \ddots & \vdots & \cdots & \vdots & \ddots & \vdots \\ a_{N_1 1}b_{N_2 1} & \vdots & a_{N_1 1}b_{N_2N_2} & & a_{N_1N_1}b_{N_2 1} & \vdots & a_{N_1N_1}b_{N_2N_2} \end{bmatrix} \quad \text{(B.7)}$$

Note that this definition can be applied to rectangular matrices as well. Consider two direct product matrices $A \otimes B$ and $C \otimes D$. If these matrices are of compatible sizes such that the products AC and BD make sense, the following identity holds.

$$(A \otimes B)(C \otimes D) = AC \otimes BD \quad \text{(B.8)}$$

The eigenvalues of a direct product matrix can be expressed in terms of the eigenvalues of the individual factors. If the eigenvalues of A (B) are denoted λ_i (μ_j), then the eigenvalues of $(A \otimes B)$ may be expressed as follows.

$$\alpha = \lambda_i \mu_j \quad \text{(B.9)}$$

Finally, the eigenvalues of any matrix squared are simply the square of the eigenvalues of the original matrix. The proof is straightforward. Consider a matrix, M, and its set of eigenvalues, λ, satisfying $M\vec{\mathrm{v}} = \lambda\vec{\mathrm{v}}$, where $\vec{\mathrm{v}}$ is the corresponding eigenvector.

$$M^2\vec{\mathrm{v}} = M(M\vec{\mathrm{v}}) = M(\lambda\vec{\mathrm{v}}) = \lambda(M\vec{\mathrm{v}}) = \lambda^2\vec{\mathrm{v}}$$

To finish this section, consider specific properties of the type of matrices encountered in developing the characteristic matrix associated with Maxwell's equations and SME. In Appendix A, the following 3-by-3 matrix $\vec{\boldsymbol{a}} \cdot \vec{\nabla}\varphi$ was introduced. Defining $\vec{p} \equiv \vec{\nabla}\varphi$, and $\mathbf{P} \equiv \vec{\boldsymbol{a}} \cdot \vec{p}$.

$$\mathbf{P} = \begin{bmatrix} 0 & -p_z & p_y \\ p_z & 0 & -p_x \\ -p_y & p_x & 0 \end{bmatrix} \quad \text{(B.10)}$$

It is fairly straight forward to prove $\det \mathbf{P} = 0$, and consequently (by Eq. (B.5)), $\det \mathbf{P}^n = 0$ for any $n > 1$. The eigenvalues of **P** are derived, where $p^2 = p_x^2 + p_y^2 + p_z^2$.

$$\det(\mathbf{P} - \lambda \mathbf{1_3}) = \det \begin{bmatrix} -\lambda & -p_z & p_y \\ p_z & -\lambda & -p_x \\ -p_y & p_x & -\lambda \end{bmatrix} = -\lambda(\lambda^2 + p^2) = 0$$

There are three distinct eigenvalues, 0, ip, $-ip$. From this result, Eq. (B.11) immediately follows, where $\boldsymbol{\Lambda}_{\mathbf{P}^2}$ represents the eigenvalue matrix of the operator $\mathbf{P}^2$.

$$\mathbf{\Lambda}_{\mathbf{P}^2} = \begin{bmatrix} 0 & 0 & 0 \\ 0 & -p^2 & 0 \\ 0 & 0 & -p^2 \end{bmatrix} \tag{B.11}$$

The specific form of $\mathbf{P}^2$ is provided in equation (B.12).

$$\mathbf{P}^2 = \begin{bmatrix} -p_y^2 - p_z^2 & p_x p_y & p_x p_z \\ p_x p_y & -p_x^2 - p_z^2 & p_y p_z \\ p_x p_z & p_y p_z & -p_x^2 - p_y^2 \end{bmatrix} = \begin{bmatrix} p_x^2 - p^2 & p_x p_y & p_x p_z \\ p_x p_y & p_y^2 - p^2 & p_y p_z \\ p_x p_z & p_y p_z & p_z^2 - p^2 \end{bmatrix} \tag{B.12}$$

A useful identity is derived for positive powers of $\mathbf{P}^2$.

$$\mathbf{P}^{2n} = (-p^2)^{n-1}\mathbf{P}^2 \tag{B.13}$$

For $n = 1$, Eq. (B.13) is clearly an identity. A result is derived for $n = 2$ after which all other results follow by repeated application of the $n = 2$ result. Since $\mathbf{P}^2$ is symmetric, one can evaluate products by multiplying columns. The algebra is demonstrated explicitly for the (1, 1) and (1, 2) entries from which the rest follow by changing index labels.

$$\begin{gathered} (\mathbf{P}^4)_{11} = (p_x^2 - p^2)^2 + p_x^2 p_y^2 + p_x^2 p_z^2 = \\ (p_x^2 - p^2)^2 + p_x^2\left(p_y^2 + p_z^2\right) = \\ (p_x^2 - p^2)^2 + p_x^2(p^2 - p_x^2) = \\ -p^2(p_x^2 - p^2) = -p^2(\mathbf{P}^2)_{11} \end{gathered}$$

$$\begin{gathered} (\mathbf{P}^4)_{12} = (p_x^2 - p^2)p_x p_y + \left(p_y^2 - p^2\right)p_x p_y + p_x p_y p_z^2 = \\ p_x p_y\left(p_x^2 + p_y^2 + p_z^2 - 2p^2\right) = \\ -p^2 p_x p_y = -p^2(\mathbf{P}^2)_{12} \end{gathered}$$

C. A VERY BRIEF INTRODUCTION TO DIFFERENTIAL GEOMETRY AND TENSORS

Parts of this section can be found in reference [4]. The intent is to provide a vocabulary list to assist the reader who is unfamiliar with some of these topics. This is by no means complete. The topic of differential geometry is commonly used in all areas of physics and engineering but for vastly different reasons. It is also approached by physicists and engineers differently than by mathematicians. A list of excellent references include the following: [12], [16], [47-50].

C.1 Metric

The metric is a generalization of the dot product and is usually introduced via a quadratic form with *dS*, a differential arc length and $a_{ij}(x_k)$ continuously differentiable functions of coordinates.

$$dS^2 = a_{ij}dx_i dx_j \tag{C.1}$$

One can always find a small neighborhood about an arbitrary point such that C.2 holds modulo constant scale factors, with $n + m = \dim(M)$, where '$\dim(M)$' refers to the dimension of the space M.

$$a_{ij} \approx \mathbf{1}_n \oplus -\mathbf{1}_m \tag{C.2}$$

When m = 0, the metric reduces to the identity matrix and the geometry is locally Euclidean. When $|n - m| = \dim M - 2$, the metric reduces to one of two choices for the Minkowski metric used in special relativity, specifically for dim(M) = 4. Manifolds with metric defined by C.1 that are locally Euclidean are referred to as Riemannian, while those that have local Minkowski geometry are termed either pseudo-Riemannian or Lorentzian.

A consequence of C.2 is that curves on a pseudo-Riemannian manifold can have positive, negative, or zero length. The coordinates of the manifold are divided into x_i, $i = 1, \dots \dim M - 1$, and t, and choosing m = 1. With this convention, curves with $dS^2 > 0$ are called space-like, and curves with $dS^2 < 0$ time-like. These two types of curves are separated by a hypersurface defined by the class of curves with $dS^2 = 0$ referred to as a null hypersurface, a generalization of the light cone.

C.2 Manifolds

A manifold, M, is an abstraction from the theory of surfaces that does not include a surrounding Euclidean space of higher dimension in its description. For a detailed definition of a manifold, see references [47-50]. I present here a few concepts used within the text. A tangent space, $T_p(M)$, is defined at each point on the manifold, which serves as an abstraction of the tangent plane to a surface. Each tangent space has the structure of flat Euclidean space, modulo constant scale factors. The metric in each tangent space, $g_{\mu\nu}(x^\alpha)$, is fixed but is allowed to vary from point to point in M. If $U, V \in T_p(M)$ then their inner product is given by $g_{\mu\nu}U^\mu V^\nu$ and $g_{\mu\nu}V^\mu V^\nu \equiv \|V\|^2$ defines the magnitude of a vector. The set of quantities, V^μ, are the components of the vector in some chosen basis of $T_p(M)$. A dual tangent space, $T_p^*(M)$, is also defined at each point of M. The metric tensor defines a mapping from $T_p(M) \rightarrow T_p^*(M)$, $T_\mu = g_{\mu\nu}T^\nu$. The T_μ are the components of the dual vector in some chosen basis of $T_p^*(M)$. Tensors of arbitrary rank are elements of a direct product space constructed of multiple copies of the tangent and dual tangent spaces $T_p(M) \times \cdots \times T_p(M) \times T_p^*(M) \times \cdots \times T_p^*(M)$. For example, the metric presented in section C1 are components of a tensor in $T_p^*(M) \times T_p^*(M)$. These spaces do not require a concept of distance to be defined. The components of a tensor of arbitrary rank are denoted $T^{\alpha_1 \cdots \alpha_N}{}_{\beta_1 \cdots \beta_M}$. A standard choice of basis for $T_p(M)$ and $T_p^*(M)$ are ∂_μ and dx^μ respectively, where x^μ are coordinates defined on an open set of M containing p. In this basis, a vector and its dual are denoted $V = V^\mu \partial_\mu$ and $V_\mu dx^\mu$ respectively.

C.3 Covariant differentiation and parallel transport

Covariant derivatives of vectors and dual vector are defined using the metric tensor.

$$D_\mu U^\nu \equiv \partial_\mu U^\nu + \Gamma^\nu{}_{\mu\alpha}\, U^\alpha, \quad D_\mu U_\nu \equiv \partial_\mu U_\nu - \Gamma^\alpha{}_{\mu\nu}\, U_\nu \tag{C.3}$$

The second term in each definition of Eq. (C.3) introduces the connection coefficient or Christoffel symbols.

$$\Gamma^{\nu}{}_{\mu\alpha} = \frac{1}{2} g^{\nu\beta}\left(\partial_{\mu} g_{\alpha\beta} + \partial_{\alpha} g_{\mu\beta} - \partial_{\beta} g_{\mu\alpha}\right) \tag{C.4}$$

The Christoffel symbols take into account the turning of the basis vectors as one differentiates the vector, requiring comparison of *V* at two points of *M*. Eq. (C.3) is a component form of the result. Comparing vectors at different points in *M* is not a trivial operation since they live in different spaces. To compare $V \in T_p(M)$ to $V \in T_q(M)$, $p, q \in M$ with $p \neq q$, one of the vectors must be moved into the space of the other. In general this requires specifying the path in space traversed by *V* from *p* to *q*, or from q to p. If T^{μ} is the velocity along the path, then *V* is parallel transported along the curve by Eq. (C.5).

$$T^{\mu} D_{\mu} V^{\nu} = 0 \tag{C.5}$$

C.4 Geodesics and the affine parameter

Geodesic curves parallel transport their velocity vector, *i.e.*

$$\frac{DT^{\nu}}{d\lambda} = T^{\mu} D_{\mu} T^{\nu} = 0 \tag{C.6}$$

When Eq. (C.6) holds, the parameter λ defined along the curve is called an affine parameter. Any other choice of parameterization will change Eq. (C.6) to the following.

$$T^{\mu} D_{\mu} T^{\nu} = \sigma T^{\nu} \tag{C.7}$$

The parameter σ is an arbitrary scalar function defined along the curve. Equation (C.7) makes the transported tangent vector “parallel” to the tangent of the curve at the new point (allowing a change in magnitude), whereas the auto-parallel condition requires the transported tangent vector to be identical to the tangent vector at the new point along the curve. For space-like geodesics, arc length is a natural choice for an affine parameter. Time-like geodesics may also be parameterized by their length interpreted as a standard internal time, or the proper time of an observer whose world line coincides with the particular time-like curve. Clearly, for null curves, arc length cannot be used as a parameter. In such cases, one imposes C.7 and the null constraint thus defining the parameter as affine with no physical significance attached (more appropriately, no physical significance is required).

Defined in Eq. (C.6) as auto-parallel, the geodesic equation is also the Euler-Lagrange equation derived from a variation of the arc length.

$$\delta \int dS = 0 \tag{C.8}$$

Equation (C.8) defines geodesics as curves of “optimal” length, either minimizing or maximizing the length between two points of *M*.

D. POLYNOMIAL CHAOS BASIS

The polynomial chaos approach makes use of orthogonal polynomials with weighting functions that match the statistics of the input parameters as closely as possible. Wiener's original paper introduced the Hermite polynomials for modeling Gaussian parameters [9]. One can express any distribution in terms of any set of orthogonal polynomials as these completely span Hilbert space. However, the right choice can make a given problem easier to solve. Generalizations of Wiener's chaos have been investigated and used in UQ problems in all areas of engineering. This section lists the known distributions and their orthogonal polynomial expansion, normalization conditions, and triple integral products used in this report as a quick reference.

Table 5 – List of common distribution and their chaos polynomial basis

Distribution	Density function	Orthogonal polynomial basis	Weight function	Domain
Normal	$\frac{1}{\sqrt{2\pi}}\exp\left(-\frac{x^2}{2}\right)$	Hermite $He_n(x)$	$\exp\left(-\frac{x^2}{2}\right)$	$(-\infty,\infty)$
Uniform	$\frac{1}{2}$	Legendre $P_n(x)$	1	$[-1,1]$
Beta	$\frac{(1+x)^\beta(1-x)^\alpha}{2^{\beta+\alpha+1}B(\alpha+1,\beta+1)}$	Jacobi $P_n^{(\alpha,\beta)}(x)$	$(1+x)^\beta(1-x)^\alpha$	$[-1,1]$
Gamma	$\frac{x^\alpha\exp(-x)}{\Gamma(\alpha+1)}$	Generalized Laguerre $L_n^\alpha(x)$	$x^\alpha\exp(-x)$	$[0,\infty)$
Exponential	$\exp(-x)$	Laguerre $L_n(x)$	$\exp(-x)$	$[0,\infty)$

The polynomials listed are orthogonal relative to the corresponding weight function but are unnormalized.

Table 6 – Orthogonality conditions and normalized chaos polynomials

Orthogonal polynomial	Orthogonality condition	Normalized polynomial
$He_n(x)$	$\int_{-\infty}^{\infty} He_n He_m \exp\left(-\frac{x^2}{2}\right)dx = \sqrt{2\pi}n!\,\delta_{nm}$	$\frac{1}{\sqrt{\sqrt{2\pi}n!}}He_n(x)$
$P_n(x)$	$\int_{-1}^{1} P_n P_m dx = \frac{2}{2n+1}\delta_{nm}$	$\sqrt{\frac{2n+1}{2}}P_n(x)$
$P_n^{(\alpha,\beta)}(x)$	$\int_{-1}^{1} P_n^{(\alpha,\beta)}P_m^{(\alpha,\beta)}(1+x)^\beta(1-x)^\alpha dx = \frac{2^\gamma}{2n+\gamma}\frac{\Gamma(n+\alpha+1)\Gamma(n+\beta+1)}{\Gamma(n+\gamma)n!}\delta_{nm}$	$\frac{1}{\sqrt{A_n^{(\alpha,\beta)}}}P_n^{(\alpha,\beta)}(x)$

$L_n^\alpha(x)$	$\int_0^\infty L_n^\alpha L_m^\alpha x^\alpha e^{-x} dx = \frac{\Gamma(n+\alpha+1)}{n!}\delta_{nm}$	$\sqrt{\frac{n!}{\Gamma(n+\alpha+1)}} L_n^\alpha(x)$
$L_n(x)$	$\int_0^\infty L_n L_m e^{-x} dx = \delta_{nm}$	$L_n(x)$

The following shorthand is used in table 6, $\gamma = \alpha + \beta + 1$, and the normalization factor $A_n^{(\alpha,\beta)}$ is obvious by inspection.

Applying polynomial chaos to a PDE often results in triple or quadruple integral products of basis functions. These can be reduced in some cases using well known product formulas and the orthogonality conditions. Product rules for Legendre, Hermite, Generalized-Laguerre, and Laguerre polynomials are provided here.

$$P_k P_l = \sum_{m=|k-l|}^{k+l} \begin{pmatrix} k & l & m \\ 0 & 0 & 0 \end{pmatrix}^2 (2m+1) P_m \tag{D.1}$$

$$H_m H_n = \sum_{r=0}^{\min(m,n)} r!\, 2^r \binom{m}{r}\binom{n}{r} H_{m+n-2r} \tag{D.2}$$

$$L_{m_1}^{(\alpha_1)} L_{m_2}^{(\alpha_2)} = \sum_{s=0}^{m_1+m_2} B_s^{(m_1,m_2)} L_s^{(\beta)} \tag{D.3}$$

$$L_m L_n = \sum_{s=0}^{m+n} B_s^{(m,n)} L_s \tag{D.4}$$

The coefficients in equation D.3 and D.4 are,

$$B_s^{(m_1,m_2)} = (-1)^s \sum_{r_1,r_2} (-1)^{r_1+r_2} \frac{(\alpha_1+1)_{m_1}(\alpha_2+1)_{m_2}}{(m_1-r_1)!\,(m_2-r_2)!\,(\alpha_1+1)_{r_1}(\alpha_2+1)_{r_2}} \frac{(r_1+r_2)!\,(\beta+1)_{r_1+r_2}}{r_1!\,r_2!\,(r_1+r_2+s)!\,(\beta+1)_s}$$

More general product formulae can be found in the references, [41-45]. The Pochhammer symbol is represented by Z_x and the 6 index factor in equation D.1 is the $3j$ symbol or Clebsch-Gordon coefficient. Triple products of polynomials, as well as general product formulas, can be found in the literature. The quadruple products for the Legendre, Hermite, and Laguerre polynomials, are presented. Bra-ket notation is used to represent the multiple products, incorporating the weight function implicitly.

$$\langle P_l|P_mP_n\rangle = \sum_{k=|m-n|}^{m+n} \begin{pmatrix} m & n & k \\ 0 & 0 & 0 \end{pmatrix}^2 (2k+1)\langle P_l|P_k\rangle = \sum_{k=|m-n|}^{m+n} \begin{pmatrix} m & n & k \\ 0 & 0 & 0 \end{pmatrix}^2 2\delta_{lk}$$

$$\langle H_l|H_mH_n\rangle = \sum_{r=0}^{\min(m,n)} r!\,2^r \binom{m}{r}\binom{n}{r} \langle H_l|H_{m+n-2r}\rangle = \sum_{r=0}^{\min(m,n)} r!\,2^r \binom{m}{r}\binom{n}{r} \sqrt{\pi}2^l l!\,\delta_{l,m+n-2r}$$

$$\langle L_l|L_mL_n\rangle = \sum_{s=0}^{m+n} B_s^{(m,n)}\langle L_l|L_s\rangle = \sum_{s=0}^{m+n} B_s^{(m,n)}\delta_{l,s}$$

In each case, the sum can be further reduced. Selection rules are determined by consistency requirements imposed by the limits of the summations as well as the nature of the coefficients within the sum. For example, the Legendre triple product contains stringent selection rules imposed by the Clebsch-Gordon coefficients. If any of the following conditions hold the triple product $\langle P_l|P_mP_n\rangle$ vanishes, $l+m+n$ is odd, $l<m+n, m<n+l, n<l+m$. The general expressions for Legendre, Hermite, and Laguerre quadruple products are listed below.

$$\langle P_kP_l|P_mP_n\rangle = 2\sum_{p=|k-l|}^{k+l}\sum_{q=|m-n|}^{m+n} (2p+1) \begin{pmatrix} k & l & p \\ 0 & 0 & 0 \end{pmatrix}^2 \begin{pmatrix} m & n & q \\ 0 & 0 & 0 \end{pmatrix}^2 \delta_{pq}$$

$$\langle H_kH_l|H_mH_n\rangle = \sum_{r=0}^{\min(k,l)}\sum_{s=0}^{\min(m,n)} r!\,2^r \binom{k}{r}\binom{l}{r} s!\,2^s \binom{m}{s}\binom{n}{s} \sqrt{\pi}2^u u!\,\delta_{uv}$$

$$\langle L_kL_l|L_mL_n\rangle = \sum_{s=0}^{k+l}\sum_{r=0}^{m+n} B_s^{(k,l)}B_r^{(m,n)}\delta_{sr}$$

To simplify the Hermite expression the following shorthand is used, $u=k+l-2r$ and $v=m+n-2s$.